CO2 Network

Case Study: ...

Tobia Wyss*[2], Amorim Leandro De Castro Amoedo Rafael †[1], Luc Girardin‡[1], and François Maréchal§[1]

[1] *Industrial Process and Energy Systems Engineering (IPESE), EPFL*
[2] *Master Student, Energy Management and Sustainability , EPFL*

January 29, 2019

ÉCOLE POLYTECHNIQUE FÉDÉRALE DE LAUSANNE

IPESE
INDUSTRIAL PROCESS AND ENERGY SYSTEMS ENGINEERING

*tobia.wyss@epfl.ch
†rafael.amoedo@epfl.ch
‡luc.girardin@epfl.ch
§francois.marechal@epfl.ch

Todo list

Abstract

Many countries and cities in the world have pledged to drastically reduce their CO2 emissions during the next decades. Given the high degree of urbanization in occidental society, district energy systems present a high potential to increase the efficiency of heating and cooling systems. The present work focuses on a specific type of district network, base on CO2 as a working fluid. Through condensation and evaporation it allows to exchange heat at low temperatures, increasing the potential of heat recovery, and thus the energy and exergy efficiency of the global system. Previous studies have shown that very high efficiencies can be reach with the use of heat pumps to supply heat to the buildings, as well as to harvest heat from environment. The aim of this work is to study the performance of such a system, based on a case study, the Eglantine district located near Lausanne. Specifically it has been looked at evaluating the integration of a geothermal field, as a heat source. The main research questions that will be tried to answer are:

How does the CO2 district energy network perform - energetically as well as financially - in the Eglantine district, harvesting heat from a geothermal field, and under which conditions does it perform better than concurrent solutions?

What are the characteristics of a typical district that favor the choice of the CO2 district energy network technology?

A comparative analysis shows that...
Conclusions here

Acknowledgments

I would like to thank prof. Marechal to have given me the opportunity to do my master thesis in his research group IPESE, on a subject and in a mindset that i appreciate a lot.

I had the chance to work with Amoedo Rafael and Luise Middelhauve, who i thank for having supervised me and, most importantly, for having given me a good support and structure. A special thanks goes to Luc Girardin for the useful and interesting discussions we had, but also for the time he accorded me and the guidance given me throughout this project.

I also thank all the doctor students and researchers at IPESE that might have answered some of my questions, or simply greeted me in the morning. It was a pleasure!

Contents

1 Introduction

1.1 Context

Throughout the last decades, human society has developed thanks to energy, most of which has come from fossil fuels. This has led to an unprecedented rise in CO2 emissions, which have proved to be at the source of climate change. In order to secure a livable planet for the years to come, it is necessary, among others, to drastically reduce CO2 emissions[?]. Since the adoption of the Kyoto protocol, the first international treaty about the fight against climate change in 1992, many countries have agreed to drastically reduce CO2 emissions in the coming decades.

One crucial sector is the production of heat, which represents a large share of the total greenhouse emissions. This is especially true for countries at higher latitudes, i.e. with cold climates. For example in Switzerland the energy demand for space heating and hot water demand of buildings, accounts for around 41% (96.5 TWh) of the total energy demand of the country, and is still strongly dependent from fossil fuels. If we also include process heat, this figure rises to 54% (123.9 TWh)[?].

Also the energy demand related to cooling is experiencing an exponential growth. This is, on the one hand, because it is becoming affordable for more people, as income levels rise. On the other hand, this increase is due to global warming, which leads worldwide to a higher average temperature, as well as an increase in the frequency of days with extreme temperatures[?]. There are today 1.6 billion air conditioners (AC) in use, and about 50% of them are distributed in only two countries: China and USA. In some countries, especially in the Middle East, as well as in parts of the USA, during extremely hot days cooling can represent more than 70% of peak residential electricity demand. A huge problem with respect to this, is the quality of ACs. The majority of ACs that are sold in large markets, have an efficiency, which is only 50% or lower than the one of the best products available. This engenders, obviously, an important augmentation of the energy demand. Figure 1 shows how the energy demand has tripled since 1990, while the share of cooling energy in total energy use in buildings has risen from 2% to more almost 7% [?].

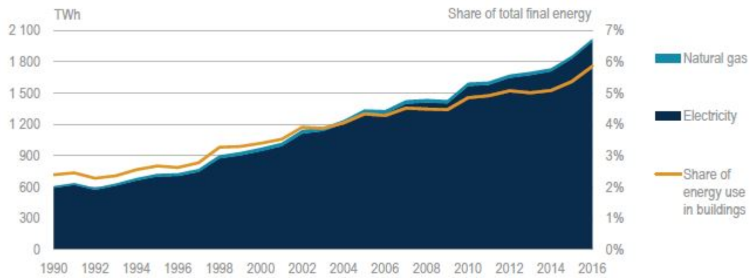

Figure 1: World energy consumption for space cooling in buildings. Source:[?]

A study shows that also in Switzerland cooling demand will strongly increase in the next decades, due to climate change. Figure 2 shows how this is particularly true for modern houses, which are very well isolated and efficient for the winter use. In this case the cooling demand will represent more or less a third of the heating demand[?].

According to the Population Division of the United Nations, the share of the world population living in cities has steadily increased from 34% in 1960 to 55% in 2017. Moreover, they prospect that, by 2050, this number will rise to 66%. In Switzerland, as well as in its neighbouring countries, the percentage of urban population is considerably higher, with 74% (2017) [?]. The fact that people live more and more in concentrated areas, also mean that the density of energy consumption is rising. This becomes particularly interesting for urban heating and cooling demand, since the high density of heat consumers sets the conditions for efficient systems, based on district energy networks.

The UNEP (United Nations Environment Programme) has identified a big potential in modern district energy systems, as the most effective approach to improve energy efficiency for heating

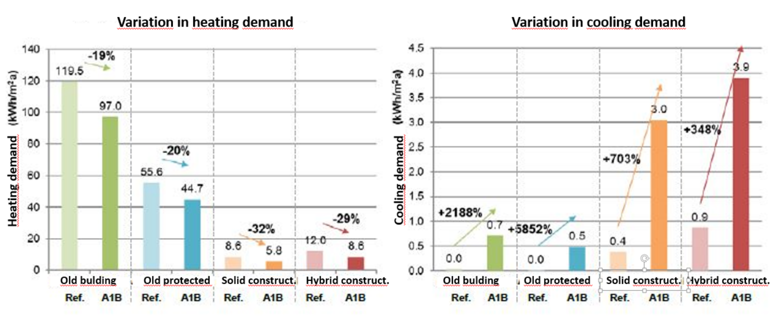

Figure 2: The evolution of median values of heating (left) and cooling (right) demand of the fours case studies ("Old building", "Old builing protected", "Solid construction", "Hybrid construction") between the reference period "1995" (1980-2009) and the period "2060" (2045-2074) in Basel. The percentage variations can be attributed to climate change. A1B corresponds to a median scenario developed by the IPCC. Source: [?]

and cooling, and enable the integration of renewable energies. However, these technologies require a high level of technology coordination and planning, since they create more efficient systems that are also more complex to deploy and operate. This is why, further research and technology development are needed in order to foster the spreading of these technologies.

1.2 Scope

The scope of this project is to pursue the study of the application of the CO2 based district energy network technology, proposed by Weber and Favrat[?]. In collaboration with Romande Energie, the utility company of canton Vaud, a feasibility study has to be performed on a specific case study: the residential district Eglantine in Morges. The work will try to answer the main research questions:

How does the CO2 district energy network perform - ecologically as well as financially - in the Eglantine district, and under which conditions does it perform better than concurrent solutions?

What are the characteristics of a typical district that favor the choice of the CO2 district energy network technology?

2 State of the art

2.1 District heating

The evolution of the technology of district heating (DH) is shown in Figure 3. The first District Heatings (DH) have been installed in the 1880s in the USA, using concrete ducts to distribute steam at high temperature, which was then condensated by the consumers. This system was obviously not very efficient, due to the elevated heat losses during transportation, as well as the exergy losses due to the high temperature level. In the early 1930 a second generation was developed, which based on the use of pressurized water, distributed above 100°C. These networks were installed with the purpose of reducing fuel consumption, as well as to integrate the energy generation through CHPs (Combined Heat and Power). The third generation was introduced in the 1980s and it's main difference was the use of a lower distribution temperature (below 100 °C). In those years the main reasons for the installation of DH was security of supply, since they allowed to replace oil with more local and cheaper fuels such as coal, biomass and waste. Moreover, it allowed to use industrial waste heat, as an energy source.

Nevertheless, a distribution temperature between 70-100 °C still origins very high heat losses, and it does not allow to integrate a larger number of heat sources. Moreover, also in space heating systems in buildings, there has been an evolution towards lower operating temperatures, reducing the average demand temperature. These were the drivers for the development of the 4th generation, for which networks operate at a temperature between 30-70 °C. This enables a much better integration of the heating system into the global energy system, as it makes it possible to include low temperature sources (geothermal, solar thermal, refrigeration systems or waste heat from data centers).

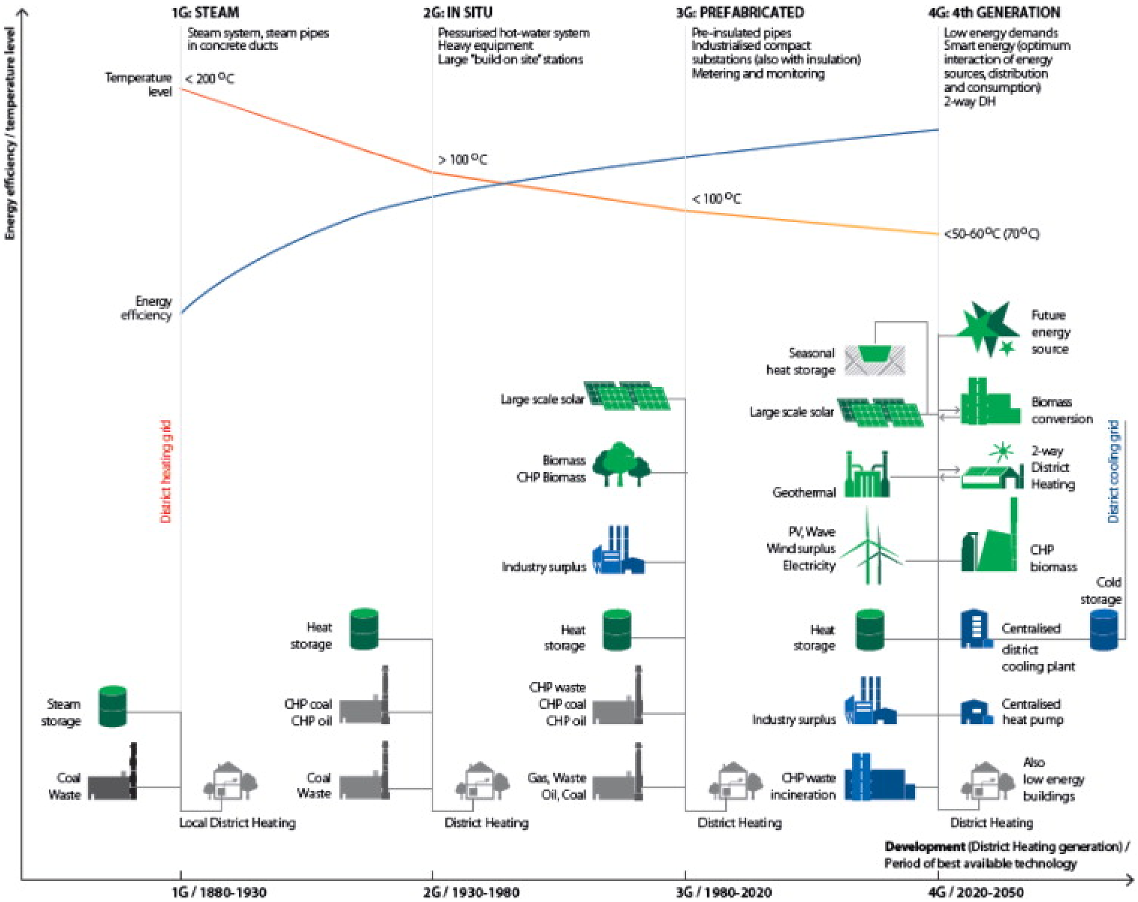

Figure 3: The evolution of the district heating technology, from the 1st to the 4th generation. Source: [?]

District cooling (DC) networks had a similar development as DH networks, although to a smaller extent.

2.2 Fifth generation district energy networks

The 4th generation of DH technology, has already achieved remarkable success and has been widely applied, especially in Europe. However, the exergy losses of the system are still very high, due to the diversity of heat levels present in the system, limiting its efficiency. Moreover, the integration of DC, which, as it was mentioned beforehand is already important in cities and will become more and more important throughout the next years, needs the installation of a second and separate networks, which leads to high upfront costs.

This has lead to the birth of a new technology that uses an even lower distribution temperature (10-25 °C) to provide heating and cooling. In fact, the transfer fluid acts as cold network for cooling purposes and supplies, at the same time, evaporator heat to decentralized heat pumps. This is what is known as the 5th generation DH networks, also known as District Energy Networks (DEN) or District Heating and Cooling (DHC). Besides the higher energy and exergy efficiency, which reduce the operating costs, this technology also reduces the upfront costs. Given the lower distribution temperature, in fact, the pipes require less insulation, as well as they can be placed in shallower depth in the ground.

This technology has appeared in Switzerland in 2007, and it's mostly known as *anergy network*, or in german *Anergienetz*. To the authors knowledge, there are seven such systems operating by the end of the year 2018[?]. A summary of a selection of four of them is shown in Table 1, while more detailed information can be found in the Appendix 7.

Table 1: District energy systems in Switzerland

	Anergienetz ETH Hönggerberg	**Suurstoffi-Areal**	**Anergienetz Friesenberg (FGZ)**	**Genève-Lac-Nations (GLN)**
Location	Zürich	Rotkreuz	Zürich	Genève
Year of construction	2012 - 2026	2010 - 2020	2011-2050	2008 - 2016
ERA [m2]	475'000	172'421	185'000	840'000
Inst. Heating capacity $[kW]$	8'000	6'732	3'930	4'300
Heating demand $[MWh/a]$	28'450	10'619	35'000	5'000
Inst. Cooling capacity $[kW]$	6'000	2'327	3'500	16'200
Cooling demand $[MWh/a]$	26'200	2'364	80'000	20'000
Distribution fluid	water	water	water	water
Heat source	Laboratories waste heat +HP	Waste heat buildings + PVT (solar th.) +HP	Waste heat data center+HP	Lake water +HP
Heat storage	Geothermal well field (431 at 200m)	Geothermal well field (215 at 150 m, 180 at 280m)	Geothermal well field (332 at 250m)	None
T of heating pipe	24 °C - 8 °C	25 °C - 8 °C	28 °C - 8 °C	17 °C - 5 °C
T of cooling pipe	4 °C - 20 °C	4 °C - 17 °C	4 °C -24 °C	5 °C - 12 °C
Tot. investments $[Mio.CHF]$	37	n/a	42.5	33
Tot. COP of heating (incl. Pumps...)	5.8	2.7	4.1	6.5

All the anergy networks presented in Table 1 still base on water as a working fluid. Therefore, they work on sensible heat, which means that a heat exchange is bound to a variation in the fluids temperature. The challenge of these systems is given by the flow rate that is necessary to limit the temperature difference between the inlet and the return temperature of the network. Thus, it could be very interesting to use refrigerants, instead of water, that enable to work with latent heat instead, which means collecting and distributing heat through the condensation, or the evaporation, of the refrigerant. This poses some additional technological challenges, but has also very clear advantages, as it will be shown in the next chapters.

The choice of the refrigerant strongly depends on the application. In function of the operating

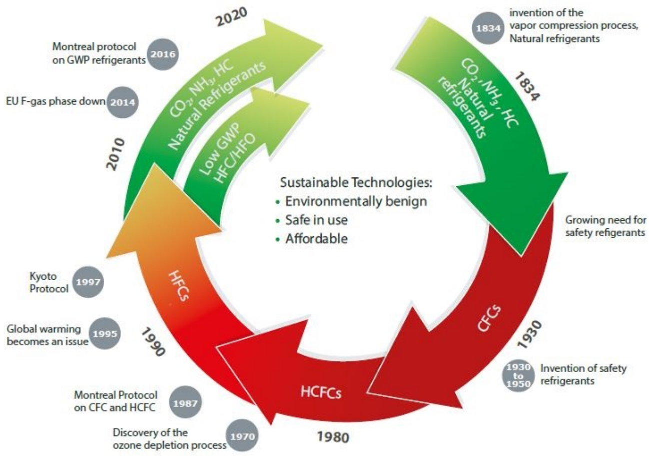

Figure 4: The historical cycle of refrigerants Source: [?]

conditions, three main criteria are evaluated: affordability, safety and environmental impact. A summary of the history of refrigerants is shown in Figure 4. The Montreal protocol, signed in 1987, designed the phase out of HCFC and CFCs, in order to prevent ozone layer depletion. This boosted the use of HFCs, as a replacement. However, not far later, people realized that despite being less damaging to the ozone layer, they were powerful greenhouse gases. Since 2013, a federal ordinance also strongly restricts the use of these last ones in Switzerland[?]. Also Europe has planned the phase-out of HFC in 2014[?]. This means that today the choice of refrigerants is essentially limited to natural refrigerants - as for example CO2 (R744), ammonia (R717) or propane (R290) - and the new environmentally friendly HFOs - as for example the fluorinated propane isomer R1234yf.

The choice of CO2 as a refrigerant relies, besides its thermodynamic properties, on the following arguments[?]:

- it is very abundant in the environment and is also waste of a multitude of industrial processes
- it is harmless to the biosphere
- it is non-flammable and non-toxic
- it is an inert gas

In fact, according to Danfoss[?], CO2 will dominate industrial refrigeration, together with ammonia. Already today, this technology is widely used. For instance Migros, Switzerland's largest retail company, opened its first supermarket to use CO2, in a low-temperature subcritical system, in 2002. By today, 411 of the 700 supermarkets in Migros's portfolio are equipped with transcritical CO2 systems[?].

2.3 CO2 DEN

2.3.1 The technology

Weber and Favrat [?] compared the performance of a DEN using subcritical CO2, the HFO R1234yf and water. They were able to show that the CO2 network performs best, and has the biggest potential for DEN systems[?]. As explained above, a refrigerant based DEN technology allows to store and transfer heat through the latent heat of vaporization of the refrigerant. The operating pressure is chosen in order to obtain the desired temperature in the system. That temperature is selected to be as high as possible to represent a good heat source for the decentralized heating heat pumps - resulting in good COP values -, while still allowing free cooling - avoiding the installation of compression chillers, and thus drastically reduce electricity consumption for space cooling.

The network consists of one saturated liquid pipe and of one saturated vapor pipe, both in a saturated temperature range from 12 to 18 °C[?]. The working principle is shown in Figure 5. Heating users can extract heat from the network through condensation of the refrigerant, taken from the vapour pipe. Respectively, cooling users take refrigerant from the liquid pipe and evacuate heat by evaporating it. The heat exchanges between the network and the users occur through condenser-evaporators heat exchangers, which keep the different refrigerant loops isolated[?]. The synergy between simultaneous heating and cooling users allows the recovery of waste heat. Most of the time, the required heating and cooling capacity will not be equal, which means that there is the need for a centralized balancing power. Indeed, a central plant is responsible to balance the overall network, by exchanging heat with the environment. For instance, a sole/water or a water/water heat pump can be used for this purpose.

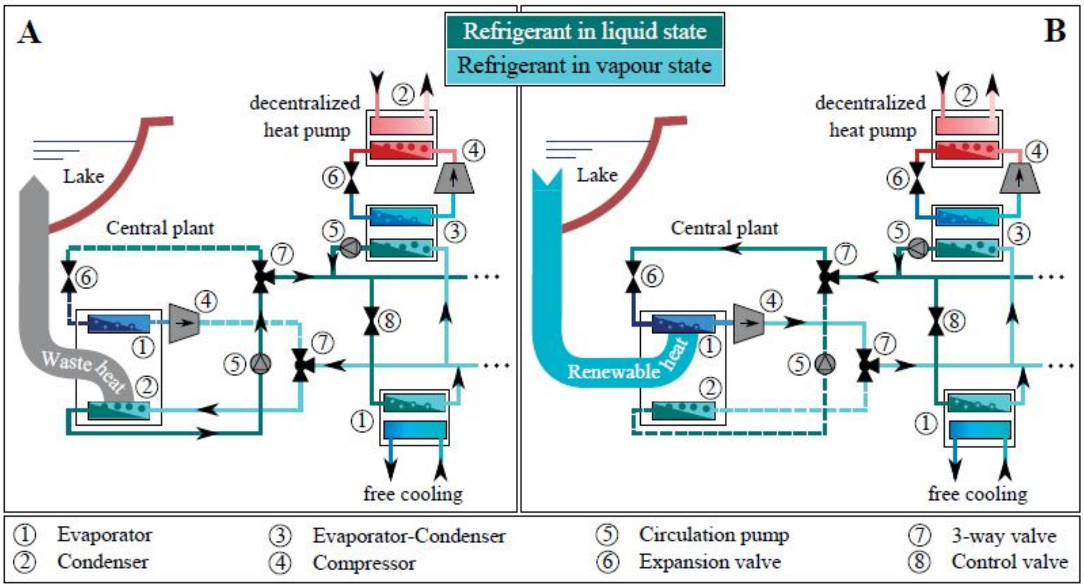

Figure 5: Schematics of a refrigerant based district energy network. Part A represents its net cooling operation, and part B its net heating operation. Source: [?]

One of the big advantages of this technology, with respect to water based DEN, is the pipes sizing. In fact, given the fact that it works on pressure maintenance instead of a fluid flow, no return pipe is necessary, which results in a slightly shorter total length of installed pipes. Moreover, due to the higher energy density of latent heat, the pipes diameter is drastically reduced. Henchoz et al. [?] compared three different working fluid on the same study case, showing that, while CO2 needs pipes of only 280/330mm (liquid/vapor), R123yf would need 270/700mm and water 625/625mm. Given the low operating temperatures, there are much lower requirements for pipes insulation. While water pipes need to be buried deep enough to prevent damage due to water freezing, in case part of the network had to be stopped during winter, CO2 does not freeze and thus does not require a minimum freeze-safe depth. Henchoz et al. have even imagined installing the pipes inside a sidewalk module, which would drastically simplify maintenance and inspection. Given the smaller diameter, it would also be possible to retrofit an old, high temperature district heating network, by placing the CO2 pipes inside the old water pipes. All the above mentioned advantages of using CO2, result in lower upfront costs.

The main drawback of this technology is the high operating pressure, which situates at about 50 bars, and the safety concerns that could derive from the large amount of CO2 that could escape in case of a major leakage. Nevertheless, as described in 2.2, CO2 refrigeration networks are already widely used in supermakets, and the technology is considered as safe.

2.3.2 Performance

Henchoz et al.[?] performed an analysis of the potential application of a CO2 based DEN in a district in the city of Geneva. A map of the district, called "Rues basses", is shown in Figure 6.

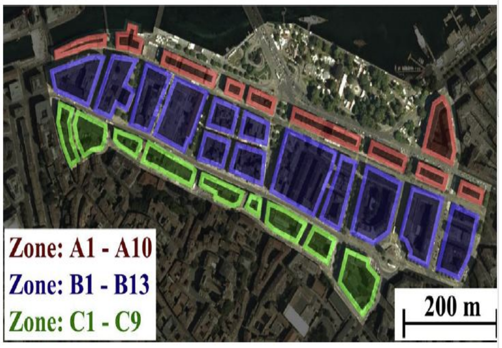

Figure 6: Representation of the the studied area and of its subdivision into 32 zones. Source: [?]

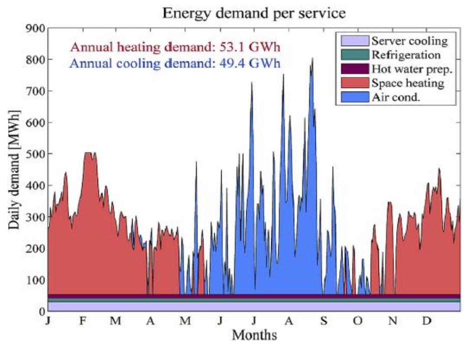

Figure 7: Energy demand for the area studied over the year 2012. Source: [?]

Table 2 shows the distribution of building affectations - which is important to determine the energy consumption - in the studied area. The total ERA is $687'800m^2$.

Table 2: Distribution of the energy reference area for the different zones and building affectations

Zones	Commercial [m^2 ERA]	Offices [m^2 ERA]	Residential [m^2 ERA]
A1 - A10	20’700	89’200	17’700
B1 - B13	97’000	260’700	61’600
C1 - C9	40’400	62’600	48’100
Relative share	23%	60%	17%

The energy demand of heating ($53.1GWh/yr$) and cooling ($49.4GWh/yr$) in the studied area is shown in Figure 7. Throughout the year, the district presents nearly the same heating demand as for cooling, but they happen in different seasons.

The proposed CO2 based DEN is balanced by a central plant - a heat pump - that exchanges heat with the nearby lake. In order to benchmark the results, this technology has been compared to a traditional heating and cooling system, based on oil boilers and cooled compression chillers.

The results are remarkable. In fact, the CO2 based DEN shows a final energy consumption of 10,968 MWh of electricity, which corresponds to a reduction of 84.4 %, with respect to the reference scenario. Its exergy efficiency situates between 40-45%.

2.3.3 Integration in smart energy system

The integration of high shares of renewable energies represents an important challenge. In fact, it requires a lot of slack to handle the volatile nature of renewable energy sources like wind or sun. On one side, this slack will be mainly given through a smart control of the electricity grid on multiple levels. It starts from the demand side management (DSM) inside households, through optimization at district level, up to a national and international control. These decentralized grids, or grid controls, are called *smart grids*.

With the vast success of heat pumps throughout the last decade, the control of electricity grids is more and more interconnected with the production of heat. This further complexifies the system by adding a level of constraints, but it also opens new levels of control. Indeed, if well designed, a

DEN offers an additional level of slack that can be used in combination with the smart grid, multiplying control power. The CO2 DEN offers several possibilities to shift the loads, relieving the grid.

On one hand, it simplifies the deployment of a smart control of the heat pumps, which can strongly contribute in the DSM. The decentralized heat pumps can make use of a buildings thermal inertia to adapt electricity use to energy availability. CO2 vapor and liquid storage can act as a buffer, enabling load-shifting also for the central plant of the DEN. Sizing of these storage capacities will determine the possible time-span that the shift can achieve. Given the low distribution temperature, this approach also facilitates the storing of heat, as for example in a geothermal field.

On the other hand, the use of CO2 as a refrigerant for the network could improve the integration of a power to gas (PtG) system. Indeed, one big challenge in the future, especially in higher latitudes, where seasonal variation are consistent, is to ensure energy supply during winter season, when, due to shorter and weaker solar irradiation, PV panels produce less. It is thus important to find a way to store the excess of renewable energy production during the summer, in order to use it in the winter. One solution to do that is PtG, which defines the process of transforming electrical power to a gas, like methane, which is easy to store. To do so, electricity is used to produce hydrogen, which can be combined with CO2 to form Methane, in a process called methanization. Methane can be used during the winter to produce electricity and heat, in a combined heat and power plant (CHP), as for example a SOFC, a gas turbine, or a combination of them. For this reason, PtG is widely studied across Europe and many such plants have already been built.
Suciu et al. [**?**] studied the synergy between a CO2 based DEN, decentralized PV and such a PtG system. The CO2 network could be used to store the carbon dioxide, which is captured from CHPs or industrial processes during winter, needed for methanization. At the same time, the DEN can directly use and dispatch the heat produced from the CHPs. In their work, they analyzed the PV area, and thus the investment, required to achieve a completely autonomous energy system, for different European climatic zones. The results showed that decarbonized autonomous energy systems based on DENs and PtG tecnologies are possible, along with a very broad deployment of solar energy. It is also shown that the payback time of such a system is between 11 and 14 years, which makes it very attractive also from an economic point of view.

2.4 Direct-expansion ground source heat pump

where to put this section?

For heat pumps based systems, sourcing heat from the sole, instead of from the ambient air, is a very interesting solution at our latitudes, especially, as it has been seen, for integration of a 5th generation DEN, since it improves heating and cooling COPs, and, to a certain extent, it allows heat storage. In traditional Ground-Source Heat Pumps (GSHP), the heat pump and the ground are connected by means of a closed loop, using water, or a water solution. This system, called the secondary loop GSHP (SL-GSHP), is shown on the right side of Figure 8. However, it has been proved [**?**, **?**] that the system efficiency can be improved, by allowing to directly expand the refrigerant into the ground and thus let the ground act as a condenser/evaporator. Shown on the left side of Figure 8, this system is called Direct Expansion GSHP (DX-GSHP).

So far, this technology is not so widely spread, mostly because of a more demanding system design and, because of the risk of environmental pollution, when non-natural refrigerants are used. Indeed, literature about DX-GSHP is still scarce, especially for CO2 as a refrigerant. The are only few numerical CO2-DX-GSHP studies [**?**, **?**, **?**, **?**], which are not yet sufficient to obtain a scientific appreciation of the technology. Nevertheless several prototypes and experimental set-ups have been built and analyzed [**?**, **?**, **?**], proving a higher efficiency of the DX, with respect to a SL.

On of the main reasons for this efficiency gain is the elimination of the temperature lift of the water loop, which is replaced by a constant temperature phase-change, as well as the elimination of the minimum approach temperature necessary to exchange heat between the SL and the heat pump. This results in a higher COP for the heat pumps. Moreover, CO2 presents a higher heat transfer coefficient, which again allows to either reduce the minimum approach temperature, or extract a higher power with respect to an equal exchange surface. The minimum approach temperature has to be determined in function of the thermal permeability of soil and is correlated to the length and total surface of the geothermal probes, as well as the refrigerant flow rate.

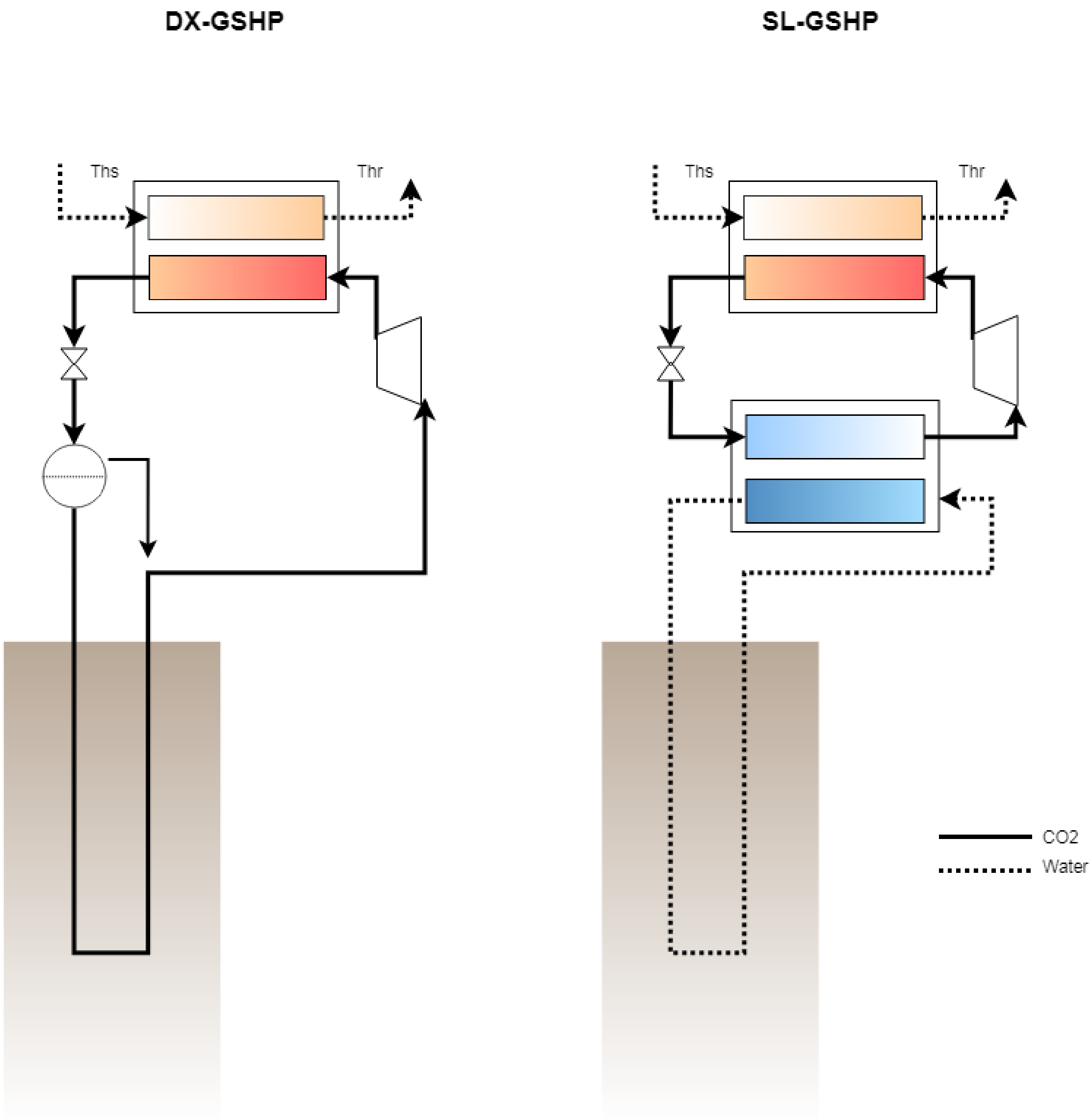

Figure 8: A simplified schematics of the two GSHP technologies

2.5 MILP and Osmose

Mixed integer linear programming (MILP) is a mathematical optimization, in which some variables are restricted to be integers, while other are discrete. A MILP model can be written with AMPL (A Mathematical Programming Language), which is a modeling language specifically designed to describe and solve optimization problems. Once defined the model, this is passed to a solver, as for example Gurobi or GLPK, which solves the given problem.

Osmose is a platform developed at IPESE for the study and the design of complex integrated energy systems. Its aim is to allow the user to model and compute an optimization problem using the same platform, which would normally require to access and transfer data between several programs. The coding language is *lua*.

Osmose allows to define a model for the different energy conversion technologies that want to be analyzed. It will then prepare the files that will be handed over to AMPL. After the solving is complete, the results are post-processed, allowing to run sensitivity analysis, multi-objective optimizations or simply calculate performance indicators.

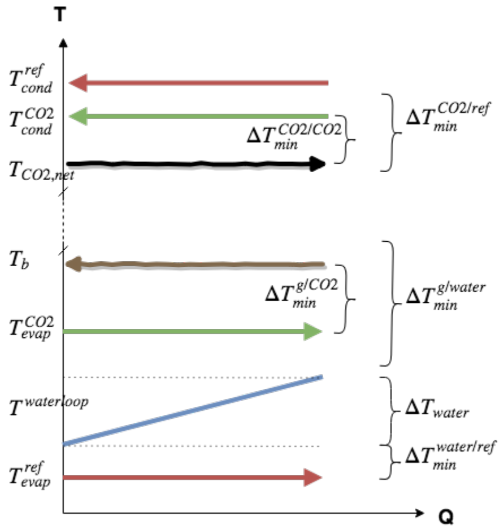

Figure 9: Schematic representation of heat exchanges and minimum approach temperatures for the central plant HP, comparing SL- and DX-GSHP

In first place, energy technologies have to be defined, with its set of equations that determine the supply and the demand of the unit. Moreover it is necessary to furnish the following cost parameters:

- cinv1: fixed part of the IC, given in $[CHF/year]$. This can be found in figure 10;
- cinv2: variable part of the IC, given in $[CHF/year]$. This can be found in figure 10;
- cop1: fixed part of the OC, which corresponds to maintenance and service costs.
- cop2: variable part of the OC. This is calculated by the solver, also in $[CHF/h]$.

The sizing of the energy conversion technologies is constrained with the following equations[**?**]:

$$f_{u,t} \leq f_u \forall \qquad \forall u \in U, \ \forall t \in T \tag{1}$$
$$f_u^{min} \cdot y_u \leq f_u \leq f_u^{max} \cdot y_u \qquad \forall u \in U \tag{2}$$
$$\tag{3}$$

For *process units*, only the houses, $y_u = f_u^{min} = f_u^{max} = 1$

A set of equations, called heat cascade, makes sure that heat is always transferred from a higher temperature to a lower one, also considering the respective minimum approach temperature for each stream.

$$\sum_u^U f_{u,t} \cdot \dot{Q}_{u,t,k} + \dot{R}_{t,k+1} - \dot{R}_{t,k} = 0 \qquad \forall k \in K, \ \forall t \in T \tag{4}$$
$$\dot{R}_{t,k} \geq 0 \qquad \forall k \in K, \ \forall t \in T \tag{5}$$
$$\dot{R}_{t,1} = \dot{R}_{t,k+1} = 0 \qquad \forall t \in T \tag{6}$$
$$\tag{7}$$

The demand $\dot{m}^+_{r,u,t}$ and the supply $\dot{m}^-_{r,u,t}$ of resource $r \in R$ of each unit $u \in U$ is computed:

$$\dot{M}^-_{r,u,t} = \dot{m}^-_{r,u,t} \cdot f_{u,t} \qquad \forall r \in R, \ \forall u \in U, \ \forall t \in T \tag{8}$$
$$\dot{M}^+_{r,u,t} = \dot{m}^+_{r,u,t} \cdot f_{u,t} \qquad \forall r \in R, \ \forall u \in U, \ \forall t \in T \tag{9}$$
$$\tag{10}$$

The balance of each resource has to be respected:

$$\sum_{u}^{U} \dot{M}^{-}_{r,u,t} = \dot{M}^{+}_{r,u,t} \qquad \forall r \in R,\ \forall t \in T \tag{11}$$

Electricity is also balanced:

$$\dot{El}^{+}_{houses} + \dot{El}^{+}_{heating} + \dot{El}^{+}_{cooling} + \dot{El}^{+}_{grid} = \dot{El}^{-}_{PV} + \dot{El}^{-}_{grid} \tag{12}$$

The optimization of a system is done in function of an objective function, which is chosen depending on the purpose. A possibility is to optimize the total cost of the system:

$$min\,(TotalCost) = min\,(CAPEX + OPEX) \tag{13}$$

$$min\,(Operatingcost) \tag{14}$$

$$min \sum_{u}^{U} \left[\sum_{t=1}^{T} \left(c_u^{op1} \cdot y_{u,t} + c_u^{op2} \cdot f_{u,t} + C_{el}^{-} \cdot \dot{El}^{-}_{grid,t} - C_{el}^{+} \cdot \dot{El}^{+}_{grid,t} \right) \cdot t_t^{op} \right] \tag{15}$$

$$\tag{16}$$

where c_u^{op1} and c_u^{op1} are the respectively the fixed and the variable operating cost, and C_{el}^{-} and C_{el}^{+} are the buying and selling price of electricity.

3 Methodology

3.1 Energy demand / Typical days

The energy demand profile is calculated as a function of the ambient temperature[?], using a threshold temperature for heating of $T_{th}^{heat} = 14°C$ and for cooling of $T_{th}^{cool} = 18°C$. Specific energy requirements per square meter in function of the typology of the building are taken from SIA standards.

The optimization of an energy system is commonly performed over the time span of one year, in order to account for the different seasons. However, this requires a very long computing time, given the high number of timesteps. Thus, it is used to group similar days, according to a set of parameters as for example temperature or irradiation, into so called typical days. The days can be clustered in different ways. It can be chosen to compute an average day for each month or some machine learning clustering algorithm - as for example K-means, DBSCAN or GMM - can be used to group the days into the desired number of clusters. The resulting typical days correspond to a period p, with a number of times t, as explained in section 2.5. In order to account for the data compression, a value called *occurrence* indicates how many times a given typical day occurs, i.e. how many times a given period occurs.

Two additional days with the two opposite extreme temperature conditions are added to the typical days, in order for the model to account for them in the equipment sizing. To avoid a bias of the operation results, those days are set with an occurrence of zero.

3.2 Geothermal wells

The most important parameter in geothermal wells is the soil temperature, which is normally constant throughout the year. In fact, only the first 10 meters are influenced by the temperature of the air[?]. Moreover, the temperature increases with depth. According to the SIA norm SIA384[?], the mean temperature in a geothermal well can be calculated by:

$$T_{g,mean} = T_{g,sup} + \frac{L_w \cdot \nabla T_g}{2} \tag{17}$$

where $T_{g,sup}$ is the ground temperature at the surface, L_w is the length of the well and ∇T_g is the temperature gradient of the soil.

As for other technologies, the energy demand of the circulating pumps is assumed to be negligible.

3.3 Investment cost function

To calculate the investment cost for a given technology, it is possible to interpolate data from available products on the market. However, it is also possible to evaluate a cost function, according to a standard procedure in industrial processes[**?**].

First, it is necessary to calculate the cost of purchase of the unit, in function of its size, given by the sizing power, which can be the electrical power E, the delivered heat Q or the area of a heat exchanger A.

$$C_{pex} = \frac{I_t}{I_{t,ref}} \cdot 10^{(k_{1,ex}+k_{2,ex}\cdot\log(E/Q/A))} \tag{18}$$

Through a factor called *Bare Module Factor*, the accessory costs of transport, installation, connection are included in the calculation, obtaining the total investment costs

$$CBM_{ex} = C_{pex} \cdot FBM_{ex} \cdot e \tag{19}$$

where e is the currency ration from USD to CHF. The annuities are calculated with the annualization factor (af) by the following formula, where n is the assumed lifetime of the equipment in years, and i the interest rate.

$$IC_{yearly,ex} = CBM_{ex} \cdot af \qquad\qquad af = \frac{i\cdot(1+i)^n}{(1+i)^n - 1} \tag{20}$$

This investment cost function is not a linear function. However, as described in Section 2.5, to solve the MILP it is necessary to provide a set of linear parameters that approximate the function. These are found by linearizing the investment cost function around the reference value, defined in the range of application. This was done with help of a matlab code, using *polyfit* and *polyval* functions. Figure 10 shows the linearized function with the according cost parameters.

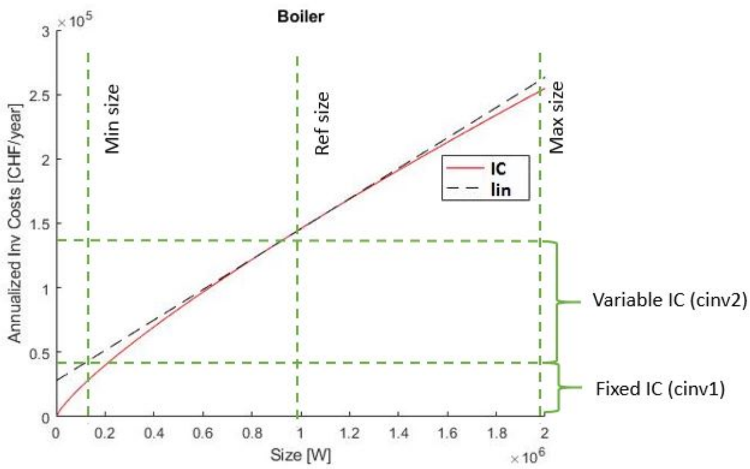

Figure 10: Linearization of investment cost function

3.4 Minimum approach temperature

The critical sizing parameter for a heat exchange is the minimum approach temperature ΔT_{min}, which corresponds to the smallest temperature difference in the heat exchanger between the hot and the cold stream, as shown in Figure 11. This value is strongly dependent from the heat exchanger area A_{ex} and the heat transfer coefficients h of the exchanging fluids. They are correlated in the following way:

$$A_{ex} = \frac{Q_{ex}}{U \cdot LMTD} \tag{21}$$

$$LMTD = \frac{(T_{Hot,in} - T_{cold,out}) - (T_{Hot,out} - T_{cold,in})}{\log\left(\frac{T_{Hot,in} - T_{cold,out}}{T_{Hot,out} - T_{cold,in}}\right)} \tag{22}$$

$$T_{Hot,in} = T_{cold,out} + \Delta T_{min} \tag{23}$$

where $LMTD$ id the logarithmic mean temperature difference and T are the inlet and outlet temperatures of the hot and cold streams, as shown in Figure 11. The overall heat transfer coefficient is given by [?]:

$$U = \frac{1}{\frac{1}{h_{(hot)}} + \frac{\Delta x_{wall}}{k_{wall}} + \frac{1}{h_{(cold)}}} \tag{24}$$

where $h_{(hot)}$ and $h_{(cold)}$ are the heat transfer coefficient of the hot and cold fluid, while Δx_{wall} and k_{wall} are respectively the thickness and the thermal conductivity of the heat exchanger plates.

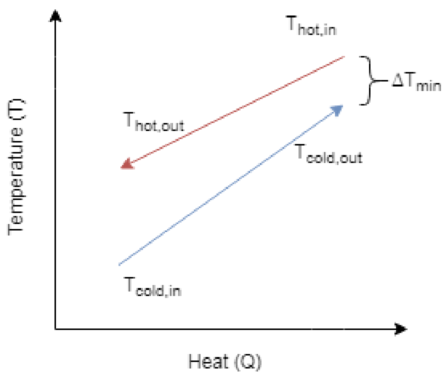

Figure 11: Minimum approach temperature in a counter-flow heat exchanger.

A bigger A_{ex} allows a smaller ΔT_{min}, which increases the investment costs but lowers the operating costs, and the other way around. Therefore, an optimum can be found for each specific application. The optimization is done by minimizing the total cost, which include the operating costs of a heat pump - whose COP decreases with ΔT_{min} -, and the investment costs of the heat exchanger and of the HP:

$$\min_{\Delta T_{min}} \{OC(\Delta T_{min}) + IC(\Delta T_{min})\} \tag{25}$$

Heat transfer coefficients used in this work are shown in Table 3. For R134yf, the heat transfer coefficient appears to be the same as for R134a[?], while for R744 experimental values are used[?, ?].

Table 3: Heat transfer coefficients found in literature

Fluid	Water	R134yf	R744
$h[W/(mK)]$	600	3000	7000

3.5 Exergy

The exergy of an energy transfer is defined as the maximum amount of work that can be extracted from it, through reversible transformations that exchange with the environment. Thus the calculation of exergy losses is a very interesting indicator to analyze a given process or system, since it expresses the quality and the efficiency with which the system operates, with respect to the maximum possible. Therefore, other as for the coefficient of performance, these values are always lower than 100 %.

The exergy value, i.e. the maximum work that can be extracted from an energy transfer, is derived from the first two thermodynamic principles, and is given by the following formula:

$$\dot{E}^{-}_{max} = \sum_i \dot{Q_i}^{+}(1 - \frac{T_a}{T_i}) + \sum_r \dot{M}^{+}_r(h_r - T_a s_r) \tag{26}$$

The exergy losses are thus given by the difference between the exergy value and the energy furnished to the system:

$$\dot{L} = \dot{E}^{-}_{max} - \sum_j \dot{E}^{-}_j \geq 0 \tag{27}$$

$$\dot{L} = (1 - \eta_{exergy})\dot{E}^{-}_{max} \tag{28}$$

In our case this can be written as:

$$\eta_{exergy} = \frac{\dot{E}q_{cold,a} + \dot{E}q_{hot,r} + \dot{E}^{-}_{grid}}{\dot{Q}q_{cold,r} + \dot{Q}_{hot,a} + \dot{E}^{+}_{grid}} \tag{29}$$

$$\dot{L} = (1 - \eta_{exergy})(\dot{E}q_{cold,r} + \dot{E}q_{hot,a} + \dot{E}^{+}_{grid}) \tag{30}$$

where $\dot{E}q$ are the exergy value of hot and cold streams, respectively above (a) and below (r) the ambient temperature. $\dot{E}^{+}_{grid}$ and $\dot{E}^{-}_{grid}$ are the electricity bought from and sold to the grid.

3.6 Energy technology models

The models for the energy technologies are adapted from an existing source code [?]

3.6.1 Heat pumps - basic (Carnot)

Heat pumps can be modeled in a simple way, using the principle of the Carnot cycle, with help of the following equations:

$$\dot{E}_{compressor} = \frac{\dot{Q}_{cond}}{COP_{real}} = \frac{\dot{Q}_{evap}}{\eta_{COP} \cdot COP_{theoretical}} \tag{31}$$

$$COP_{theoretical,heating} = \frac{T_h}{T_h - T_c} \qquad COP_{theoretical,cooling} = \frac{T_c}{T_h - T_c} \tag{32}$$

where $\dot{Q}_{cond}$ is the heat delivered and $\dot{Q}_{evap}$ the heat sourced by the heat pump. η_{COP} is an experimentally defined efficiency to account for irreversibility of the cycle, i.e. to give the ratio between the theoretical and the real COP. The values used in this work are shown in Table 4, calculated by Girardin et al.[?], based on values obtained from c heat pump certification center[?].

3.6.2 Heat pumps - detailed (Thermodyn.)

Given the comparison between new and efficient technologies, the differences of performance are relatively small and it might be necessary to provide a more accurate model of the heat pumps, that are able to correctly represent and calculate the operating cycles and conditions. This can be done by modeling the thermodynamic cycle[?], represented in Figure 12:

Table 4: Theoretical efficiency factor for COP

Type	Size	η_{COP}
Air/Water	Decentralized	0.34
CO2/Water	Decentralized	0.43
Ground/Water	Decentralized	0.43
Ground/Water	Centralized	0.55
Water/Water	Centralized	0.55

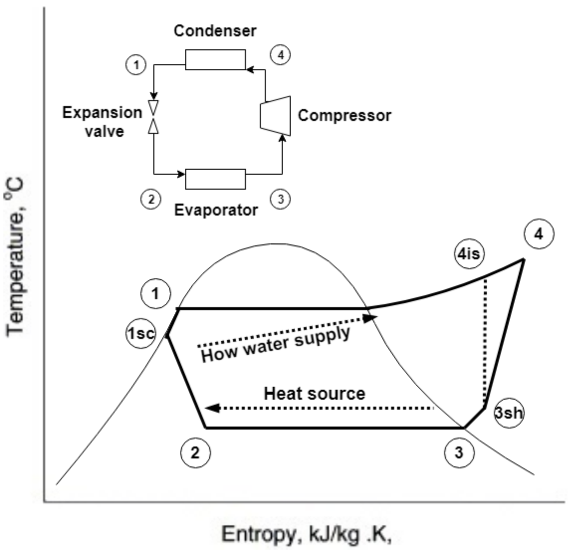

Figure 12: Temperature–entropy diagram of a R134yf based heat pump system.

1 - 2 : Expansion to low pressure level

2 - 3 : Evaporation by cooling down the heat source

3 - 3sh : Superheating in evaporator

3sh - 4 : Compression to high pressure level

4 - 1 : Condensation of refrigerant, delivering heat

The compressor is a crucial component for the design of a heat pump, since it has the largest share of impact on the energy efficiency. To calculate its efficiency, the model of Hu et al.[**?**] has been used. The shaft power can be computed in function of the isentropic efficiency (η_{is}) by:

$$W_{shaft} = \frac{\dot{m}(h_{d,is} - h_s)}{\eta_{is}} \tag{33}$$

where $h_{d,is}$ is the isentropic discharge enthalpy and h_d is the suction enthalpy. The compressors input power is expressed in function of its mechanical efficiency (η_{is}) by:

$$E_{comp} = \frac{W_{shaft}}{\eta_{mech}} \tag{34}$$

The efficiency of the compressor is thus calculated as:

$$\eta_{comp} = \frac{\text{isentropic work of compression}}{\text{actual work of compression}} = \frac{\dot{m}(h_{d,is} - h_s)}{E_{comp}} = \eta_{is}\eta_{mech} \tag{35}$$

The numerical values of those efficiencies are strongly dependent from the ratio between the pressure of discharge P_d and the pressure of suction P_s of the compressor.They can be computed inside the model with help of the relations obtained by Li et al.[?]:

$$\eta_{mech} = 0.85 \tag{36}$$

$$\eta_{is} = 0.874 - 0.0134 \cdot (\frac{P_d}{P_s}) \tag{37}$$

$$\tag{38}$$

The expansion of the refrigerant in the expansion valve is assumed to be isenthalpic.

Thus, the procedure to evaluate the operating conditions of the heat pump is the following:

1. calculate thermodynamic state in point (1) knowing the evaporation temperature T_{evap} and assuming saturated liquid
2. calculate thermodynamic state in (1sc) using same pressure as in (1), with $T = T_{evap} - \Delta T_{subcool}$
3. calculate thermodynamic state in point (3) knowing the evaporation temperature T_{cond} and assuming saturated vapor
4. calculate thermodynamic state in (3sh) using same pressure as in (3), with $T = T_{cond} + \Delta T_{superheat}$
5. calculate thermodynamic state in (2), assuming isenthalpic expansion of the valve, with $H_2 = H_{1sc}$ and P_3
6. calculate isentropic efficiency of compressor $\eta_{c,is}$, knowing the discharge pressure P_1 and the suction pressure P_3
7. calculate thermodynamic state in (4is), assuming an isentropic compression with S_{3sh} and P_1
8. calculate thermodynamic state in (4), accounting for the isentropic efficiency of the compressor $\eta_{c,is}$, using $H_4 = H_{3sh} + \frac{H_{4is} - H_{3sh}}{\eta_{c,is}}$, and P_{1sc}.

In Osmose, these values are calculated with help of *Coolprop*, which is an open-source database of fluid and humid air properties that allows to calculate operating conditions for a large number of fluids and refrigerants. Thanks to a *lua wrapper*, which is a *lua* module that provides an API to the external software, *Coolprop* is called inside Osmose.

The electrical power of the heat pump and its COP, are then calculated by:

$$E_{el} = \frac{m_{ref} \cdot (H_4 - H_{3sh})}{\eta_{mech}} \tag{39}$$

$$Q_{cond} = m_{ref} \cdot (H_4 - H_{1sc}) \tag{40}$$

$$COP = \frac{Q_{cond}}{E_{el}} \tag{41}$$

where m_{ref} is the massflow of refrigerant in the heat pump.

3.6.3 Heat pump - supercritical CO2

In traditional heat pumps, the heat delivery occurs through condensation of the refrigerant, which happens at a fixed temperature. This originates high exergy losses, especially in processes were a high temperature lift is needed in the gas cooler. Some refrigerants have the particular property of having a very low critical point. Among others, a very interesting one is CO2 - technically know as R744 -, which has a critical point at 74 bars and 31 °C[?]. As explained in Section 2.2, CO2 is also a very interesting choice for environmental and financial reasons.

The supercritical cycle is shown in Figure 13, represented on the temperature-entropy diagram. The different steps of the process are explained hereafter:

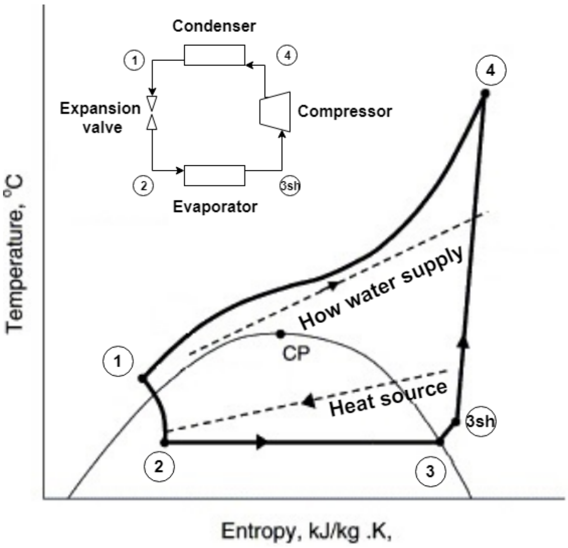

Figure 13: Temperature–entropy diagram of a trans-critical CO2 heat pump system for a domestic hot water production. Source: [?]

1 - 2 : Expansion to low pressure level

2 - 3 : Evaporation by cooling down the heat source

3 - 3sh : Superheating in evaporator

3sh - 4 : Compression to transcritical pressure

4 - 1 : Gas cooling in transcritical area, to heat water

Note that, as there is no phase change, the heat exchanger is called gas cooler, instead of condenser.

Even though the technological development is slowly closing the gap, CO2 compressors have lower isentropic efficiency and lower volumetric efficiency than subcritical ones[?]. This comes from the high irreversibility caused by the superheated vapor horn and the high throttling losses[?]. However, transcritical operation also allows heat to be exchanged on a varying temperature, and the heat pump can be designed to fit the heat demand stream, optimizing exergy efficiency. This is particularly interesting in exchanges that require high temperature lifts, as in the case of domestic hot water heaters. In fact, this can be seen in Figure 13, between point 2 and 3. For instance, Stene et al. show that COP for a CO2 HP is lower if it is used in subcritial range - for Space Heating (SH) (35/30 °C) - than in supercritical range - Domestic Hot Water (DHW) (10/60 °C) -, despite the much higher temperature difference. They also show that the resulting COP for DHW application outperforms conventional HPs[?].

For the transcritical CO2 heat pump, the numerical values of the compressor efficiencies computed with help of the relations obtained by Wang et al [?]:

$$\eta_{mech} = 0.64107 + 0.07487 \cdot (\frac{P_d}{P_s}) \tag{42}$$

$$\eta_{is} = 0.8014 - 0.04842 \cdot (\frac{P_d}{P_s}) \tag{43}$$

$$\tag{44}$$

The procedure to evaluate the operating conditions of the heat pump is the following:

1. calculate thermodynamic state in (1) with help of the temperature at the outlet of the condenser $T = T_{cond,out} = 15.5$°C, optimized for this specific cycle by Henchoz et al.[?], and

the pressure $P_{cond,out} = 84.9bar$, optimized to satisfy the required inlet temperature of the condenser

2. calculate thermodynamic state in point (3) knowing the evaporation temperature T_{evap} and assuming saturated liquid
3. calculate isentropic efficiency of compressor $\eta_{c,is}$, knowing the discharge pressure P_1 and the suction pressure P_3
4. calculate thermodynamic state in (4is), assuming an isentropic compression with S_{3sh} and P_1
5. calculate thermodynamic state in (4), accounting for the isentropic efficiency of the compressor $\eta_{c,is}$, using $H_4 = H_{3sh} + \frac{H_{4is}-H_{3sh}}{\eta_{c,is}}$, and $P_{cond,out}$.
6. calculate thermodynamic state in (2), assuming isenthalpic expansion of the valve, with $H_2 = H_1$ and P_3

The equations to calculate electrical power of the heat pump and its COP, are the same as in Section 3.6.2.

3.6.4 Cooling tower / Air cooler

A cooling tower is an equipment used to cool down a stream through the ambient air. This is used for example in air conditioning systems, to evacuate the heat into the environment. It consists of a set of fans that blow the air through a heat exchanger. These fans originate a parasitic power consumption that can be calculated with help of the following equation[**?**]:

$$\dot{E_{fans}} = \frac{0.605 \cdot \dot{Q}_{cond}}{(\Delta T_{air} + \Delta T_{min}^{ref/air})^{0.9937}} \tag{45}$$

Where $\dot{Q}_{cond}$ is the heat to be dissipated in the environment by the condenser.

3.6.5 Geo-cooling

Geo-cooling is the use of fresh temperatures of the ground for space cooling. This happens by simply circulating a fluid between the buildings, where the heat is extracted, and the geothermal wells, where heat is released into the ground. In practice, this happens by bypassing the heat pumps and making the water of the secondary loop (geothermal loop) directly exchange with the heating water loop. Investment costs are, thus, limited to an additional heat exchanger. As for the other units, the energy needed for circulation pumps is assumed to be negligible.

3.6.6 PV

The efficiency of the PV panels η_{PV} is given by the following equation[**?**]:

$$\eta_{PV} = \eta_{ref} - \eta_{var}(T_{panel} - T_{ref}) \tag{46}$$

where η_{ref} and η_{var} are respectively the fixed efficiency and the temperature dependent efficiency. The temperature of the panel T_{panel} is calculated by means of:

$$T_{panel} = \frac{U_{glass} \cdot T_{amb} + GI \cdot f_{glass} - \eta_{ref} - \eta_{var} \cdot T_{ref}}{U_{glass} - \eta_{var} \cdot GI} \tag{47}$$

where U_{glass} is the thermal transmittance of the front glass, f_{glass} is the light transmittance of the front glass and GI is the global irradiation. Thus, the produced energy is given by:

$$E = GI \cdot A_{PV} \cdot \eta_{PV} \tag{48}$$

The area of installed PV A_{PV} is limited by the maximum available roof area multiplied by the area factor f_{area}, which for flat roofs is assumed to be $\frac{1}{4}$:

$$A_{PV} = A_{roof} \cdot f_{area} \tag{49}$$

3.6.7 Network

The length is calculated, according to a simplified method[?], with the following equations:

$$L = 2(n_b - 1)K\sqrt{\frac{S}{n_b}} \tag{50}$$

with S being the land area, n_b the number of buildings. The constant K is chosen at 0.5. And diameter of the pipes:

$$d = \sqrt{\frac{4 \cdot \dot{m}}{\pi v_s \rho}} \tag{51}$$

assuming a sizing velocity v_s of 3 m/s. The investment costs are calculated accordingly:

$$C = \sum_{k=1}^{n_b} \frac{L}{n_b}(c_1 d\sqrt{n_b + 1 - k} + c_2) \tag{52}$$

where $c_1 = 5670$ and $c_2 = 613$.

Operating temperature is assumed to be 13/15 °C. Henchoz[?] has 10-12.5 for summer and 22.5 for winter!!!

how has this temperature been chosen? is there a paper? see henchoz with other T

The pressure losses, and thus the energy needed for the maintaining of the pressure, are assumed to be negligible.

4 Application

4.1 Case-study Eglantine

In the framework of the collaboration between Romande Energie and IPESE, a case study shall bring a concrete numerical case study into the discussion. For this, Romande Energie has chosen a real life example of a district in the city of Morges. This district is in the planning phase, and Romande Energie had worked on it, in order to participate in the call for tender. This case study shall be fertile ground to discuss the CO2 DEN technology and it's role in the future energy systems in Switzerland and, more particularly, in the future plans of Romande Energie.

4.1.1 Context

The "Eglantine" is a terrain in the western part of the city of Morges, as shown in Figure 14. It is located in proximity of the key urban facilities, as well as it is close to the countryside. This terrain, which was partly used for agriculture, and partly covered by rich vegetation, belongs to the municipality, who is planning to use it for the urban expansion. At the municipality, they had the vision of building a new district, which would be planned to be exemplary in the sustainable development. After many years of revising and fine-tuning the land-use plan and its vision for the future, in the beginning of 2016, the commune launched a call for tender for the planning of the different aspects of the district. The call for tender regarding the energy system was opened by Losinger Marazzi the 1st December 2017, with a due date the 31 January 2018. The contract with the winner, unknown to the author, has been signed in the end of March 2018.

The call for tender requires the development of a complete energy system, including thermal and electrical energy. Estimated data about the buildings is provided, as seen in Table 5. Those are based on the following assumptions:

- All buildings are certificated Minergie 2017
- Space heating and hot water energy demand follow the SIA 380/1 and SIA 2031 norms
- Air ventilation is defined according to Minergie 2017 principles.
- Installed power values are calculated according to SIA 2024 norm

Figure 14: Localization of the terrain, at the town scale. Source: www.geo.vd.ch

4.1.2 Buildings

The district, which will host around 1'500 people, is composed of thirteen buildings, as shown in Figure 15, which account for a total energy reference area (ERA) of around $47'000m^2$. The details are shown in Table 5. According to the Minergie standard, the district will require about $1.40MWh/yr$ for SH and $0.95MWh/yr$ for DHW.

Table 5: Estimated energy demand in call for tender

Building	**Energy Ref. Area (ERA)**	**Inhabitants**	**Space Heating (SH)**	**Hot Water (DHW)**	**TOTAL**
			MIINERGIE simple flux	SIA 380/1	
	[m2]		[kWh/yr]	[kWh/yr]	[kWh/yr]
1	8'200	273	245'180	170'833	416'013
2	2'615	76	82'308	50'104	132'412
3	2'415	70	76'328	45'938	122'266
4	2'780	92	83'122	57'917	141'039
5	3'700	116	113'246	74'306	187'552
6	1'500	50	44'850	31'250	76'100
7	2'870	83	90'652	54'653	145'305
8	2'500	83	74'750	52'083	126'833
9	4'225	140	126'328	88'021	214'349
10	4'455	148	133'205	92'813	226'018
11	4'190	139	125'281	87'292	212'573
12	2'300	76	68'770	47'917	116'687
13	2'300	76	68'770	47'917	116'687
14	2'300	76	68'770	47'917	116'687
TOT	**46'350**	**1'498**	**1'401'559**	**948'958**	**2'350'521**

The call for tender includes also information about the end use of the buildings, which is shown in Table 6. It can be seen that the buildings include, beside the residential use (multidwelling), also a small share of retail and restaurant services use, which are associated with different energy needs. Moreover, there is even a small indoor swimming pool, located in building one.

The energy profile of the buildings is calculated according to Minergie standard, as well as the SIA norms. Given the annual energy demand for space heating and hot water, as shown in Table 5, the monthly profile is shown in Figure 16.

4.1.3 Pre-studies

Some pre-studies have been commissioned by the land-owner, in order to give, on an indicative basis, the sizing of the energy system. These studies have been realized by external engineering firms and the results are contained in the call for tender. The studied parameters include the sizing for heat pumps, geothermal wells, as well as PV, and are shown in Table 7. They estimate a PV potential on the building roofs of $570kWp$, and the need for an installed heating power of $1'258kW$, using 77 geothermal wells of an average length of $271m$

4.1.4 Calculations/Energy demand/Typical days

write section eglantine calculations/energy demand

- typical days resulting profile
- cooling demand deduced from SIa or minergie
- ...

Figure 17, including occurrencies.

Figure 15: Map of the planned Eglantine district

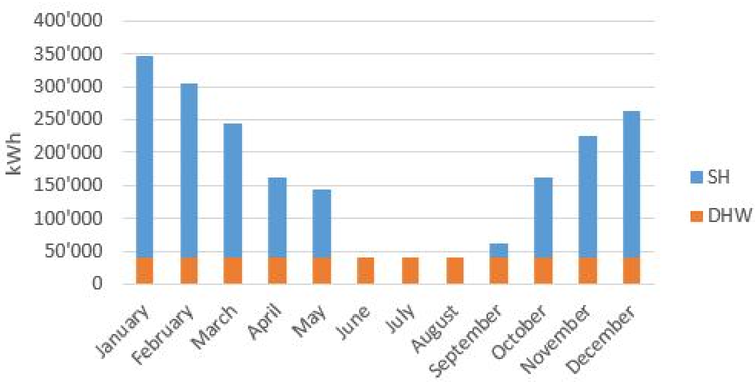

Figure 16: Annual energy distribution for space heating and hot water

Table 6: Estimated use of buildings in call for tender

Building	**Housing** [%]	**Retail** [%]	**Restaurant services** [%]	**Indoor swimming pool** [%]
1	89.58%	3.10%	4.42%	2.89%
2	97.54%	2.46%	0.00%	0.00%
3	100.00%	0.00%	0.00%	0.00%
4	100.00%	0.00%	0.00%	0.00%
5	93.19%	6.81%	0.00%	0.00%
6	95.79%	4.21%	0.00%	0.00%
7	95.79%	4.21%	0.00%	0.00%
8	100.00%	0.00%	0.00%	0.00%
9	100.00%	0.00%	0.00%	0.00%
10	100.00%	0.00%	0.00%	0.00%
11	100.00%	0.00%	0.00%	0.00%
12	100.00%	0.00%	0.00%	0.00%
13	100.00%	0.00%	0.00%	0.00%
14	100.00%	0.00%	0.00%	0.00%
Tot	97.08 %	1.63 %	0.78 %	0.51 %

Table 7: Estimated sizing of energy system in call for tender

Building	**HP** [kW]	**PV** [kWp]	**Geothermal** **Nb. wells**	**Depth** [m]
1	46	223	13	284
2	45	70	4	291
3	35	64	4	269
4	33	76	5	250
5	49	100	6	276
6	55	41	3	225
7	55	77	5	256
8	37	68	4	281
9	66	115	7	271
10	0	121	7	286
11	59	114	7	269
12	33	63	4	259
13	32	63	4	259
14	27	63	4	267
TOT	**570**	**1’258**	**77**	

4.2 Heat sources

The heat pumps in a system can source heat from various sources. Depending on the case, it is more convenient to use one or the other, given the varying temperatures and investment costs.

4.2.1 Stream

A small stream flows along the eastern boundary of the area, on which the Eglantine district is being built. The official numbers of the canton Vaud [?] are shown in Figure 18, in which the Temperature and the water flow are plotted. These values represent the average over a period of several years (7 for the temperature, and 12 for the flow rates).

According to this graph, it could be thought of using this river as a heat source for the heat

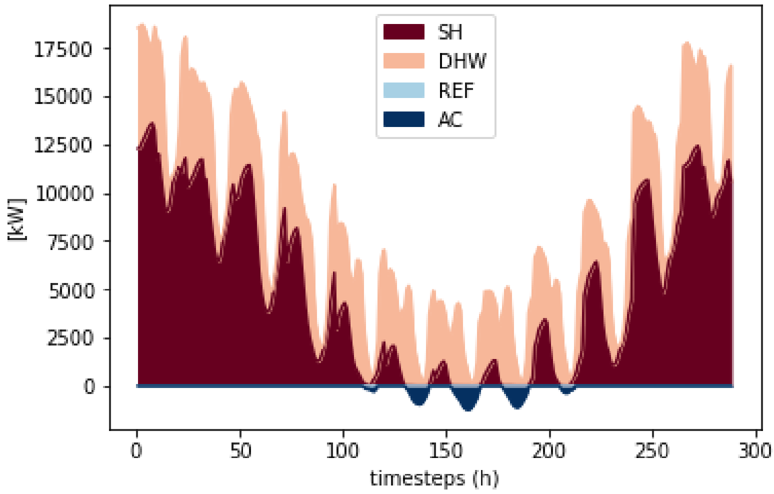

Figure 17: Total energy demand of the Eglantine district

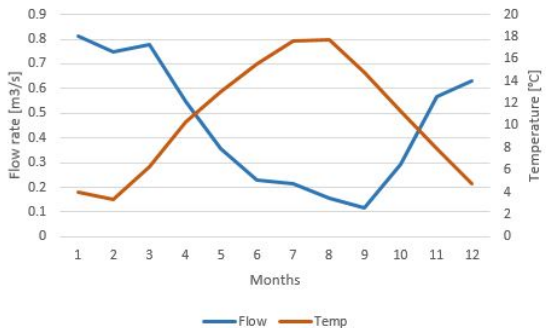

Figure 18: Temperature and flow of the Morges river

pumps. However, what is not displayed is the minimum values. In fact, during droughts, the flow rate would not be sufficient to cover the heating/cooling demand. In fact, the lowest value has been reached in August 2004 with $0.017m^3/s$, and even in December 2005 the lowest daily flow was of $0.057m^3/s$.
For this reason, the stream has been excluded from further analysis and has not been considered as a viable solution.

4.2.2 Lake

Through a pipe, the water is pumped from the lake, at a depth of around 70 m, to the central plant, located in the district area.

The massflow of the water is calculated in order to satisfy a drop/rise in the water stream of $\Delta T_{water} = 4°C$.

The cost function is calculated as for the CO2 pipes (see Section 3.6.7), considering the needed diameter to satisfy the heating/cooling demand, which depend on the different heat capacity and massflow of the water.

4.2.3 Geothermal wells

The average temperature of a geothermal well is calculated according to Section 3.2. The temperature gradient in the lemanic region is found in experimental data from the canton Geneva[**?**]:

$$\nabla T_g = 0.03[K/m] \tag{53}$$

This value also corresponds to the average gradient found in the Swiss plateau[?].

The average surface temperature depends mainly on the latitude and on the altitude. Standard values for different regions of Switzerland can be found in the SIA norm 384[?]. Experimental measurements[?] show that the surface temperature in the lemanic region is:

add images of gradient and surface temperature from PGG report?

$$T_{g,s} = 11°\text{C} \tag{54}$$

Knowing the average depth of the geothermal wells, which is found to be $L_{gtw} = 267$ (see Section 4.1), the mean temperature in the geothermal well corresponds to:

$$T_{g,mean} = 15°\text{C} \tag{55}$$

It is assumed that the geothermal wells are well sized, in order to respect the natural recharge rate, which is strongly dependent on the type of soil. The sizing of the boreholes is very important to ensure a sustainable use of the ground heat throughout the years.

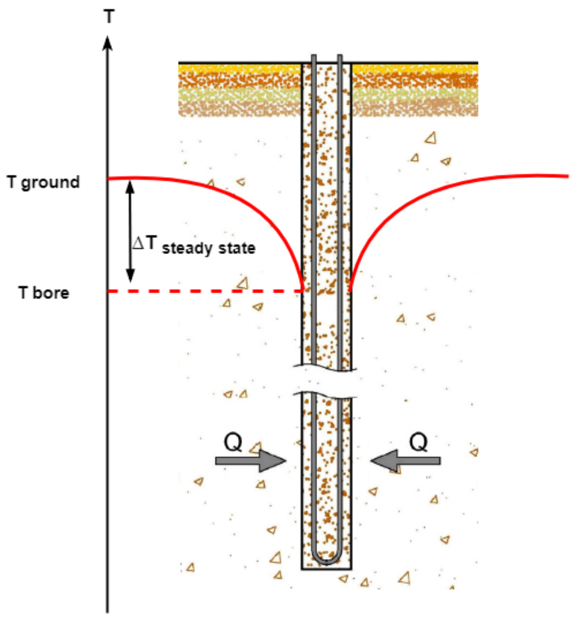

Figure 19: Steady state temperature difference in borehole, due to heat extraction

Nevertheless, there is a temperature gradient that will form around the borehole at any time heat is extracted, as shown in Figure 19, in the steady state that depends of the heat extraction rate and the conductivity of the soil. It has to be noted that this temperature gradient would be positive during heat dissipation. However, this is not in the scope of this work and it has been chosen to assume a negative temperature difference ($\Delta T_{steadystate}$) of 3 °C [?, ?], due to the reduced cooling demand for this application. Thus the mean useful temperature of the borehole over its depth is given by:

$$T_{b,mean} = T_{g,mean} - \Delta T_{SteadyState} = 12°\text{C} \tag{56}$$

The minimum approach temperature necessary to exchange heat with the soil can be determined with help of the procedure described in Section 3.4.

The price for boreholes in Switzerland is found to be around $80CHF/m$ [?]. Assuming a typical pipe diameter of $32mm$[?, ?], the corresponding cost of the heat exchange area of the borehole calculated.

To perform the ΔT_{min} optimization, the overall heat transfer coefficients of the well - including the fluid, the bore wall and the soil - are assumed to be[?]:

$$U^{g/water} = 9.3kW/m^2K \qquad U^{g/CO2} = 17.1kW/m^2K \tag{57}$$

The resulting minimum approach temperatures in ground heat exchanges are:

$$\Delta T_{min}^{g/water} = 14°\text{C} \qquad \Delta T_{min}^{g/CO2} = 6.8°\text{C} \tag{58}$$

These values are similar to experimental or standard values found in literature [?, ?].

The water rise/drop in the water ground loop is assumed to be $dT_{water} = 4°\text{C}$ [?]

The price for boreholes in Switzerland is found to be around $c_{wells} = 80$ [CHF/m] [?]. In order to provide the model with an energy dependent cost function, this value is transformed with help of the data from Table 7:

this cost function here?

$$L_{wells}^{tot} = n_{wells} * L_{well}^{average} \tag{59}$$

$$\text{Cost function [CHF/kW]} = c_{wells} \frac{L_{wells}^{tot}}{P_{hp}^{tot}} \tag{60}$$

where L_{wells} is the length and n_{wells} the number of boreholes, and P_{hp} is the total power of heat pumps installed.

inv cost is given by the Qwinter-Qsummer

4.3 External heat sources

The main advantage of a 5th generation district heating network is the ability to recover heat, and exchange it among the diversity of user. In the case of the Eglantine project, inside the district there are only very small heat sources and it is thus necessary to identify potential heat sources, located in the surroundings. Two potential heat sources have been identified in the surroundings of the Eglantine district: the ice rink and a shopping mall. For the scope of this work, only the ice rink has been considered and studied.

4.3.1 Ice rink

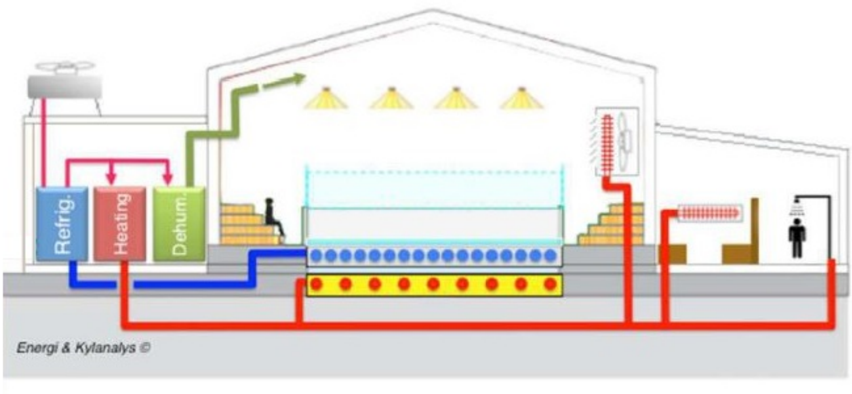

Figure 20: Energy system of a typical ice rink [?]

An ice rink is a place where people can ice skate and play winter sports. The ice surface is normally inside an arena, which ensures comfortable temperatures for the people on the ice, as well as for the public, throughout the season. This also allows to extend the season, avoiding ice melt, when temperatures are warmer outside.

A study, conducted on more than one hundred ice rinks in Sweden, shows that the refrigeration system used to cool the ice surface has the largest share in total energy consumption, 43% (in average) as indicated in Figure 21 [?]. However, the ice rink often also includes changing rooms with showers, and a cafeteria or a restaurant, which also present heating demand. According to Figure 21, the average share of heating in the total energy demand is 26%. Last but not least, the ice surface has to be constantly illuminated, which requires a powerful lightning system. The global system is shown in Figure 20.

However, for practicality reasons, it is assumed that only the refrigeration system is connected to the CO2 network, while the heating and electricity demand is supplied by the existing system, and are thus not considered in this model.

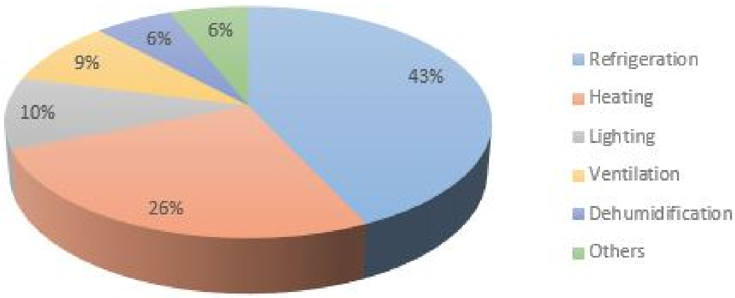

Figure 21: Energy demand of a typical ice rink [?]

Ice rinks are conventionally cooled with indirect systems, as shown in the right part of Figure 22, based on a ammonia (NH3) vapor compression chiller, exchanging with a secondary brine loop that extracts the heat from the ice surface. The waste heat is normally, or at least in older systems, exchanged with the environment, with help of cooling towers. Connecting it to a 5th generation district heating network, would allow recovering this heat and use it to cover the heat demand of other users. The connection to the CO2 network is shown in the left part of Figure 22. This presents a high energy and exergy efficiency gain, since the refrigeration system can be driven on a lower and constant condensation temperature.

The calculation of the cooling demand of the ice rink is based on the following assumptions:

- Constant load profile throughout the ice season
- Ice season: 1st of August - 1st of April
- $COP_{ref} = 4$ [?]
- Total waste heat $= 450MWh/year$ [?]
- $dT_{min}(refrigerant - ice) = 1$°C
- $dT_{min}(refrigerant - refrigerant) = 3$°C

The daily cooling demand profile of the ice rink, is based on the required ice temperature, which varies throughout the day[?], as shown in Table 24. Thus the computed ice cooling load profile is shown in Figure 23.

4.4 Variants / Scenarios

4.4.1 Heating

The heating demand is supplied by a set of decentralized geothermal heat pumps, one for domestic hot water and one for space heating in every building. These heat pumps source the ambient heat from a secondary loop that exchanges heat with the ground through a system of geothermal wells, the SL-GSHP, which is described in Section 2.4.

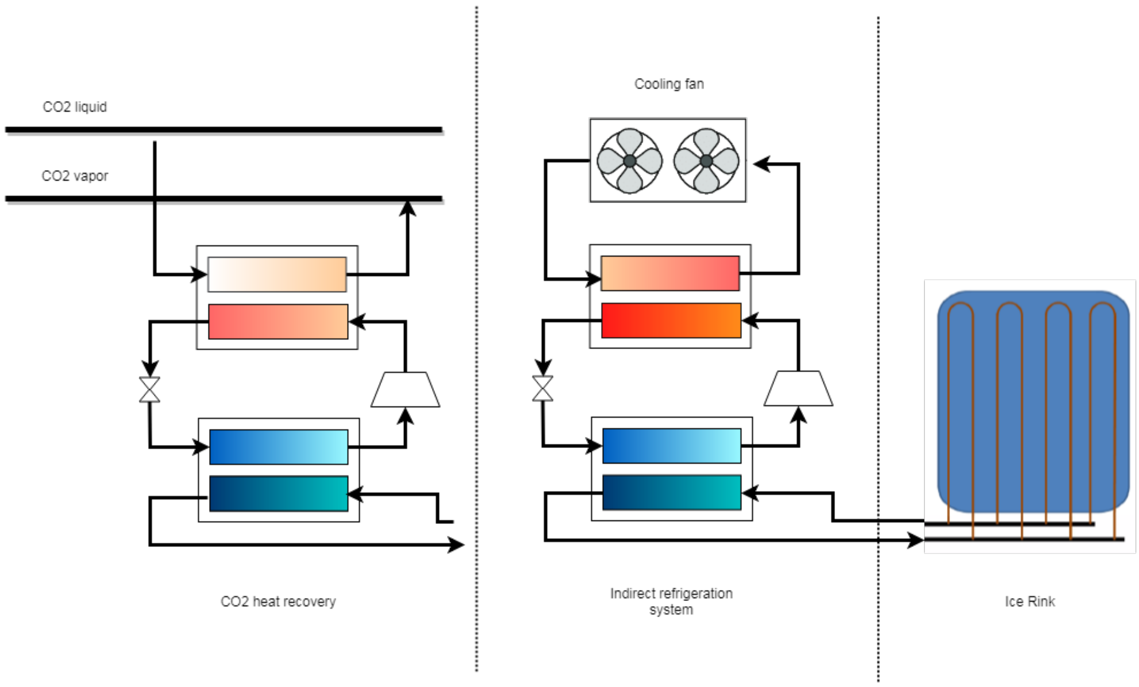

Figure 22: Refrigeration systems for ice rinks

Period	Rink function	T_{ice} [°C]
0.00-6:00	Night setback	-1
6:00-8:00	Ice maintenance	-1
8:00-16:00	Low load	-3
16:00-18:00	Figure skating	-4
18:00-24:00	Hockey	-6

Figure 23: Ice rink refrigeration profile

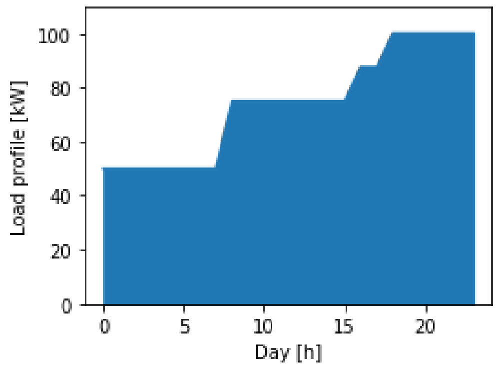

Figure 24: Ice cooling load profle of the ice rink, for a typical day

Given the relevance of the heat pumps in the studied energy system, it has been chosen to use its thermodynamic model, which achieves more reliable and precise results.

The temperatures at the evaporator and condenser are given by the following equations:

$$T_{evap} = T_{ground} - \Delta T_{min}^{ground/water} - \Delta T_{water} - \Delta T_{min}^{ref/water} \tag{61}$$

$$T_{cond} = T_{demand} + \Delta T_{min}^{ref/water} \tag{62}$$

where ΔT_{min} are the corresponding minimum approach temperatures, and ΔT_{water} is the temperature rise in the secondary water loop exchanging with the ground.

For the space heating heat pump, the refrigerant used is R123yf, as described in Section 3.6.2.

For the domestic hot water, it is chosen to use transcritical CO2 heat pumps. As described in Section 3.6.3, this technology can achieve very good performances supplying heat that requires a high lift. This is the case in domestic hot water, where the water has to be heated from a temperature of 10 °C to a temperature of 55 °C.

4.4.2 Cooling

Given the availability of geothermal wells, it has been chosen to implement geo-cooling for space cooling. The system is providing cooling at the ground temperature, corrected with the minimum approach temperature $\Delta Tmin_{ground/water}$ and the temperature rise in the water loop ΔT_{water}.

$$T_{geo-cooling} = T_{ground} + \Delta T_{min}^{ground/water} + \Delta T_{water} \tag{63}$$

4.4.3 Refrigeration

The refrigeration is achieved with a set of decentralized air cooled vapor compression chillers, which present the same working principle as heat pumps. Given that energy demand for refrigeration is not as relevant in the case study, it has been chosen to use the basic Carnot cycle model, as explained in Section 3.6.1. The heat is evacuated into the environment with help of cooling towers, as described in Section 3.6.4.

Thus, the total energy consumption is a sum of the energy demand of the compressor and the cooling fans.

$$\dot{E} = \dot{E}_{ref} + \dot{E}_{fans} \tag{64}$$

and the operating temperatures are defined in the following way:

$$T_{cond} = T_{amb} + \Delta T_{air} + \Delta T_{min}^{ref/air} \tag{65}$$

where T_{amb} is the ambient temperature, ΔT_{air} is the temperature difference of the cooling air between the input and the output of the condenser, while $\Delta T_{min}^{ref/air}$ is the minimum approach temperature difference needed for heat transfer between a refrigerant and air.

4.5 Reference scenario

In order to evaluate the potential of alternative energy systems, a reference scenario is defined. Data about the energy system that will be built in the Eglantine district is not available to the author, and therefore a standard state of the art system is used. It is assumed that the heat demand for space heating and domestic hot water is provided by decentralized geothermal sourced heat pumps. The cooling demand is provided by air cooled vapor

chillers, also commonly known as air conditioners. The scenario foresees the installation of PV panels on the roof of the buildings.

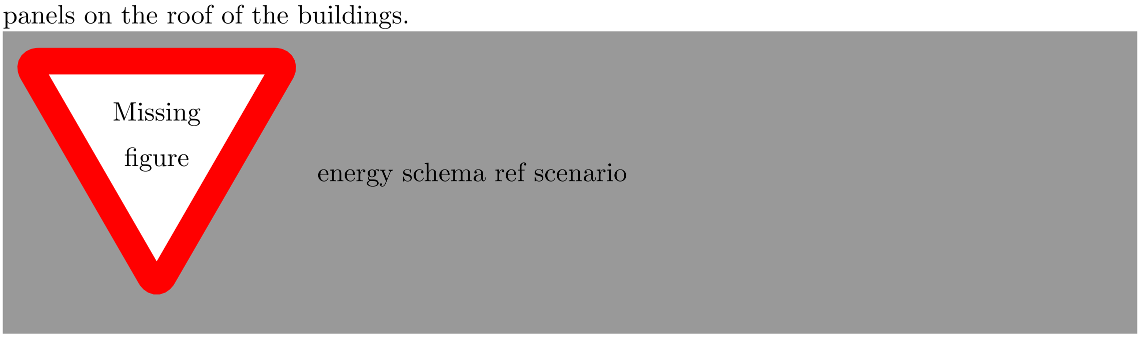

The main resource flows are shown in Table 8.

4.5.1 Heating

The heating demand is supplied by a set of decentralized geothermal heat pumps, one for domestic hot water and one for space heating in every building. These heat pumps source the ambient heat from a secondary loop that exchanges heat with the ground through a system of geothermal wells, the SL-GSHP, which is described in Section 2.4.

Table 8: Resource flows for the reference energy system ((-): flow in / (+): flow out))

	Resource flows		
Units	Electricity	$Source_{hot}$	$Source_{cold}$
HP_{sh}	-	-	+
HP_{dhw}	-	-	+
HP_{ref}	-	+	-
HE_{ac}		+	-
Elec. Heater	-		
PV	+		
GTW_{winter}		+	-
GTW_{summer}		-	+

Given the relevance of the heat pumps in the studied energy system, it has been chosen to use its thermodynamic model, which achieves more reliable and precise results.

The temperatures at the evaporator and condenser are given by the following equations:

$$T_{evap} = T_{ground} - \Delta T_{min}^{ground/water} - \Delta T_{water} - \Delta T_{min}^{ref/water} \tag{66}$$

$$T_{cond} = T_{demand} + \Delta T_{min}^{ref/water} \tag{67}$$

where ΔT_{min} are the corresponding minimum approach temperatures, and ΔT_{water} is the temperature rise in the secondary water loop exchanging with the ground.

For the space heating heat pump, the refrigerant used is R123yf, as described in Section 3.6.2.

For the domestic hot water, it is chosen to use transcritical CO2 heat pumps. As described in Section 3.6.3, this technology can achieve very good performances supplying heat that requires a high lift. This is the case in domestic hot water, where the water has to be heated from a temperature of 10 °C to a temperature of 55 °C.

4.5.2 Cooling

Given the availability of geothermal wells, it has been chosen to implement geo-cooling for space cooling. The system is providing cooling at the ground temperature, corrected with the minimum approach temperature $\Delta Tmin_{ground/water}$ and the temperature rise in the water loop ΔT_{water}.

$$T_{geo-cooling} = T_{ground} + \Delta T_{min}^{ground/water} + \Delta T_{water} \tag{68}$$

4.5.3 Refrigeration

The refrigeration is achieved with a set of decentralized air cooled vapor compression chillers, which present the same working principle as heat pumps. Given that energy demand for refrigeration is not as relevant in the case study, it has been chosen to use the basic Carnot cycle model, as explained in Section 3.6.1. The heat is evacuated into the environment with help of cooling towers, as described in Section 3.6.4.

Thus, the total energy consumption is a sum of the energy demand of the compressor and the cooling fans.

$$\dot{E} = \dot{E}_{ref} + \dot{E}_{fans} \tag{69}$$

and the operating temperatures are defined in the following way:

$$T_{cond} = T_{amb} + \Delta T_{air} + \Delta T_{min}^{ref/air} \tag{70}$$

where T_{amb} is the ambient temperature, ΔT_{air} is the temperature difference of the cooling air between the input and the output of the condenser, while $\Delta T_{min}^{ref/air}$ is the minimum approach temperature difference needed for heat transfer between a refrigerant and air.

4.6 CO2 DEN

CO2 network energy system showed in Figure...

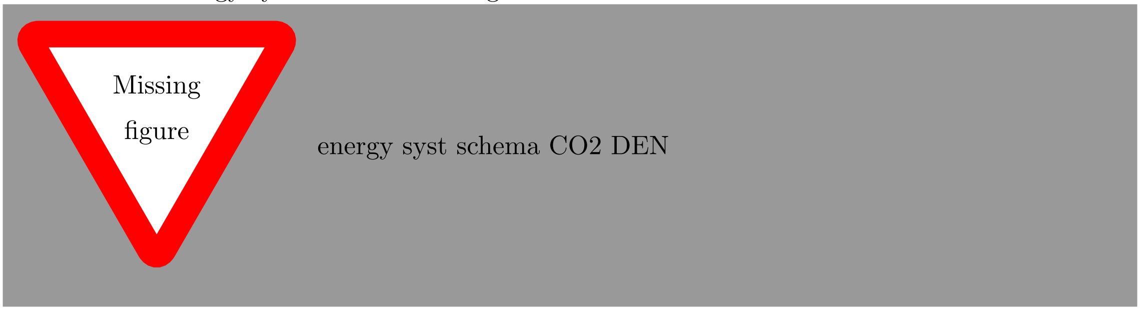

The main resource flows are shown in Table 9.

Table 9: Resource flows for the CO2 DEN ((-): flow in / (+): flow out))

-	Resource flows				
Units	Electricity	$CO2_{liq}$	$CO2_{vap}$	$Source_{hot}$	$Source_{cold}$
HP_{cp}^{winter}	-	-	+	-	+
HP_{cp}^{summer}		+	-	+	-
HP_{sh}	-	+	-		
HP_{dhw}	-	+	-		
HP_{ref}	-	-	+		
HE_{ac}		-	+		
Elec. Heater	-				
PV	+				
GTW_{winter}				+	-
GTW_{summer}				-	+

4.6.1 Heating

For space heating and domestic hot water, the same model as for the heat pumps in reference scenario are used. Sicne in this case the HP sources heat from the CO2 network instead of the geothermal wells, the mayor difference lies in the evaporation temperature, which corresponds to temperatuer in the CO2 vapor pipe ($T_{CO2,g}$):

$$T_{evap} = T_{CO2,g} - \Delta T_{min}^{ref/ref} \tag{71}$$

4.6.2 Refrigeration

As for the reference scenario, refrigeration is achieved through decentralized vapor compression chillers. However, in this case they are not air cooled, but they exchange directly with the CO2 network. Thus, the temperature in the condenser is given by:

$$T_{cond} = T_{CO2,l} + \Delta T_{min}^{ref/CO2} \tag{72}$$

4.6.3 Cooling

Free cooling has been modeled by a simple heat exchanger that evaporates saturated liquid CO2, which is then injected back into the network in a superheated vapor state with $\Delta T_{superheating} = 1K$. The mass flow of the CO2 is adapted to satisfy the cooling demand. It is assumed that pressure and temperature losses are negligible.

4.6.4 Central plant

As mentioned before, for obvious reasons, heating and cooling loads in the system are not always balanced. Thus, there is the need for a central plant to balance out the system, able to heat and cool. A centralized heat pump is very suitable for this purpose.

Equations and modeling are the same as for the above described heat pumps. Difference consists in heat source, and thus evaporation temperature. Different options have been studied:

- River: as for the lake, river water can be an interesting source of heat, with the difference of seasonal fluctuations. During the winter, river water can have a temperature close to 0, while in the summer it can rise to more than 20 °C. In the case of the Eglantine district, there is a small stream, called Morges, that passes at the eastern border of the land.

- Lake: sourced from a certain depth, lake water shows an almost constant temperature of around 7.5 °C throughout the year. This solution can be very interesting alternative to geothermal wells, since, if close enough, it might reduce the upfront costs, despite probably slightly increasing the operating costs. In this particular case, the distance to the lake is of 1500 m.

- Geothermal wells: after a certain depth, the ground presents a constant and very interesting temperature throughout the year. This heat can be exchanged with help of a secondary loop or through direct expansion of the refrigerant into the ground coils.

Direct expansion system is assumed (see Section 2.4). So the CO2 DEN with DX-GSHP technology is shown in Figure 25

explain lake=ref, geoth=DHX CO2

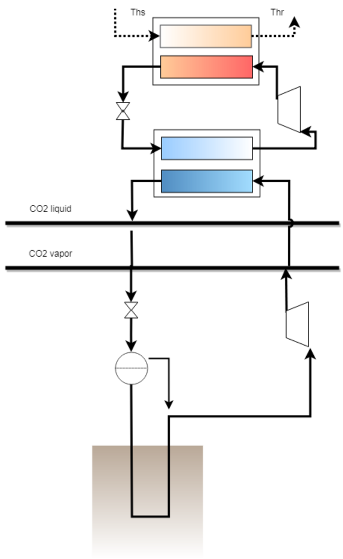

Figure 25: A simplified schematics of the CO2 DEN with DX-GSHP technology

The operating temperatures are calculating the following way.

$$T_{evap} = T_{source} - \Delta T_{min}^{CO2/source} \tag{73}$$

The operating pressure is calculated with help of *Coolprop*. The results are shown in Table 10.

summary table needed here (Ts, dTmin, Tevap, P...)? wrong values now

4.7 Values...

4.7.1 Cost functions

As described in Section 2.5, the model need investment cost parameters that can be calculated with the procedure explained in Section 3.3.

Table 10: Operating conditions for direct expansion of CO2 in heat source

Source	$\Delta T_{min}^{ref/source}$ [°C]	T_{source} [°C]	T_{evap} [°C]	P_{CO2} [bar]
Lake	4	7.5	3.5	38.2
Geothermal	10	11	1	35.8

Values for the heat pumps are given in Henchoz et al., obtained by linearizing commercial products[?]. The cost function for heat exchangers has been interpolated in order to have a function dependent on the amount of exchanged heat.

Table 11: Summary of the the investment cost function of each technology, including their expected lifetime and the interest rate.

Technology	Cost function [Euro]	X [unit]	Interest rate	Lifetime
HP	1'240 X + 5680	E_{comp} [kW]	0.08	20
heat exchanger	215 X + 56	Q [kW]	0.08	20
Electric heater	23 X + 968	Q [kW]	0.08	20
PV	300 X	A [m^2]	0.08	20
Geothermal wells	2890 X + 5800	Q [kW]	0.03	50
Network	See Section 3.6.7			

Values are summarized in Table 11.

Operating costs are calculated through the exchange with the electricity grid using the following values:

$$c_{el}^{+} = 0.2[Euro/kWh] \qquad c_{el}^{-} = 0.1[Euro/kWh] \tag{74}$$

It has also to be noted that for the scope of this work it has been assumed that the fixed part of the operating costs is negligible.

4.7.2 Minimum approach temperature

As seen in Table 3, CO2 (R744) has a higher heat transfer coefficient than other conventional refrigerants, as for example R1234yf. This has to be taken into account in the energy system through a different minimum approach temperature. To do so, there are two possible approaches:

- calculate a new, lower, ΔT_{min}^{R744}, maintaining the same heat exchange area A_{ex}. This results in higher COP for the heat pump and thus lower operating costs OC_{hp}
- calculate a new, smaller, heat exchange area A_{ex}, maintaining the same ΔT_{min}. This leads to lower upfront costs IC_{ex}

It is chosen to use different ΔT_{min}^{R744}, maintaining the same heat exchange area. The following procedure is repeated for the various fluids (X) the refrigerants have to exchange with:

1. Calculate $U_{R1234yf/X}$ with Equation 24
2. Optimize $\Delta T_{min}^{R1234yf/X}$ with numerical values from the Eglantine district, as described in Section 3.4
3. Calculate $U_{R744/X}$
4. Solve Equation 21 in function of ΔT, using $U_{R744/X}$ and the A_{ex} resulting from the previous step.

Table 12: Minimum approach temperatures used for heat exchanges in the model

ΔT_{min} [K]	Ground	Water	R744	R1234yf
Water	14	-	-	-
R744	6.8	3.46	0.8	-
R1234yf	-	4	1.4	2.3

The implementation of this algorithm has been solved on *Matlab* with help of function *solve(equation 21, ΔT_{min})*. Thus resulting ΔT_{min} values shown in Table 12.

As example, Figure 26 and Figure 27 show the resulting optimization of the minimum approach temperatures, respectively for refrigerant and ground heat exchanges. The straight line shows the optimum ΔT_{min} for the reference heat exchange, in function of the total costs (green line), while the dashed line shows the improved ΔT_{min} for CO2, maintaining the same A_{ex}.

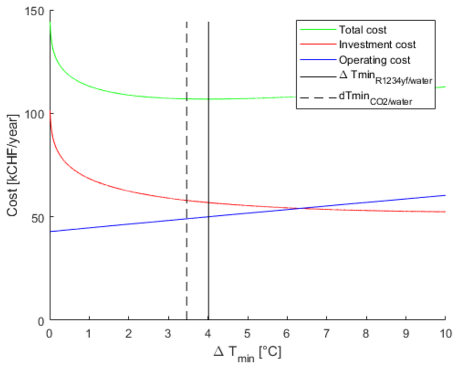

Figure 26: Optimization of ΔT_{min} values for heat exchange with refrigerant R1234yf, through minimization of total costs (green line)

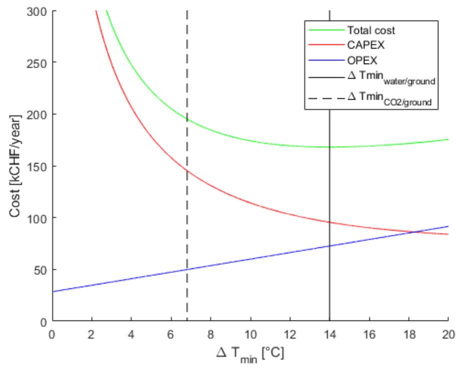

Figure 27: Optimization of ΔT_{min} values for heat exchange with the ground, through minimization of total costs (green line)

4.7.3 Compressor efficiencies

The compressor efficiencies are directly calculated in the model, according to the equations in Section 3.6.3 and 3.6.2. could be directly implemented in model. Table 13 shows the resulting efficiencies in standard operating conditions, for the different heat pumps used in this work.

Table 13: Calculated efficiencies for heat pump compressors

-	CO2 DEN					Reference scenario		
Unit	CP	CP	SH	DHW	REF	SH	DHW	REF
Refrigerant	R123yf	CO2	R123yf	R744	R123yf	R123yf	R744	R123yf
P_d	5.0	43.0	9.4	84.9	5.0	9.4	66.0	11
P_s	2.4	20.2	4.6	46.7	2.80	2.4	30.4	2.4
η_{mech}	0.85	0.80	0.85	0.78	0.85	0.85	0.80	0.85
η_{is}	0.85	0.70	0.85	0.71	0.85	0.82	0.70	0.81
η_{comp}	0.72	0.56	0.72	0.55	0.72	0.70	0.56	0.69

These values are similar to reference values found by Yang et al.[?] in their experimental work.

4.8 CP with if conditions

not sure where to put that...

In order to have a HP model for the central plant, which is able to handle different source temperatures, different cases have been implemented, with help of if conditions. Indeed, computation problems arise when the source temperatures reaches the condensation temperature of the heating part of the CP, which corresponds to the temperature of the CO2 network. In the same way, this higher source temperature also precludes the possibility of free-cooling. However, if the temperatures is higher than the CO2 network, the central pump might be able to source heat without operating a heat pump (free-heating).

The model includes two operating modes for each part of the central plant, the heating part (CP-winter) and the cooling part (CP-summer). The thresholds are set in the following way:

$$T_{thresh}^{free-cooling} = T_{CO2} - \Delta T \quad (75)$$

$$T_{thresh}^{free-heating} = T_{CO2} + \Delta T \quad (76)$$

where ΔT is the minimum temperature difference needed for the specific heat exchange.

The truth table is shown in Table 14.

Table 14: Truth table to determine if the CP operates in heat pump (HP) or in heat exchanger (HE) mode, depending on the borehole temperature and the threshold temperatures for free-cooling T^{FC} and free-heating T^{FH}

$T_{borehole}$	$\leq T^{FC}$	$T^{FC} \leq T \leq T^{FH}$	$\geq T^{FH}$
CP-winter	HP	HP	HE
CP-summer	HE	HP	HP

The parameters that vary through the if conditions are the electricity consumed E_{cp} and the investment cost parameters.

4.9 DX Vs. SL-GSHP

As discussed in Section 2.4, there is the possibility to directly expand the CO2 into the geothermal well, instead of exchanging with help of a secondary water loop. The different temperature levels are shown in Figure 28.

Results of simulation, show the difference in performance, 15.

Table 15: Comparison of simulation results for a SL-GSHP, versus a DX-GSHP

-	SL-GSHP R1234yf	DX-GSHP R744
T_{source}^{lm}	12	12
T_{demand}^{lm}	15	15
T_{cond}^{lm}	16.4	15.8
T_{evap}^{lm}	-9.4	5.2
COP_{real}	6.5	15.8
η_{COP}	65 %	60 %
η_{exergy}	6.8 %	16.6 %

CO2 heat pump has lower efficiencies (see Table 13) thus η_{COP} but much lower temperature difference to cover. Thus, its real coefficient of performance, as well as the exergy efficiency, are clearly higher than for the SL-GSHP. In fact, the DX-GSHP results being about twice as good.

It has to be noted that this specific heat pump globally presents very low exergy values. This is due to ratio between the relatively high minimum approach temperatures and the very low temperature difference between the source temperature T_b and the heat demand temperature T_{vap}^{CO2}.

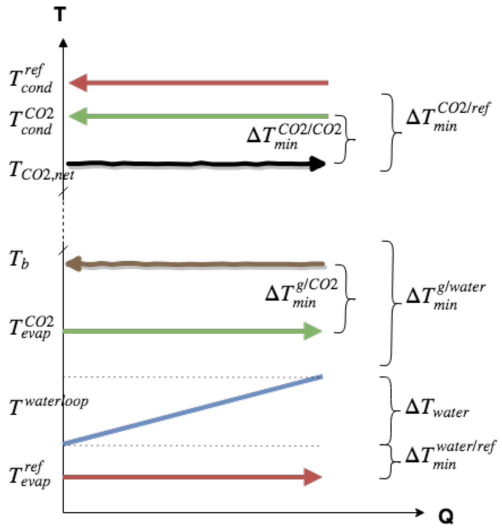

Figure 28: Schematic representation of heat exchanges and minimum approach temperatures for the central plant HP, comparing SL- and DX-GSHP

4.10 Model improvement - thermodyn cycle

Comparison of results with simple Carnot model and with thermodyn model. Show difference in COPs

Recalculation of η_{COP} for all ETs. From the real COP calculated with help of coolprop and the thermodynamic cycle of the heat pump, the COP efficiency can easily be calculated

$$\eta_{COP} = \frac{COP_{real}}{COP_{theoretical}} \tag{77}$$

Table with new eta cop values.

COP Comparison with values from literature?

5 Results and discussion

5.1 Energy and exergy performance

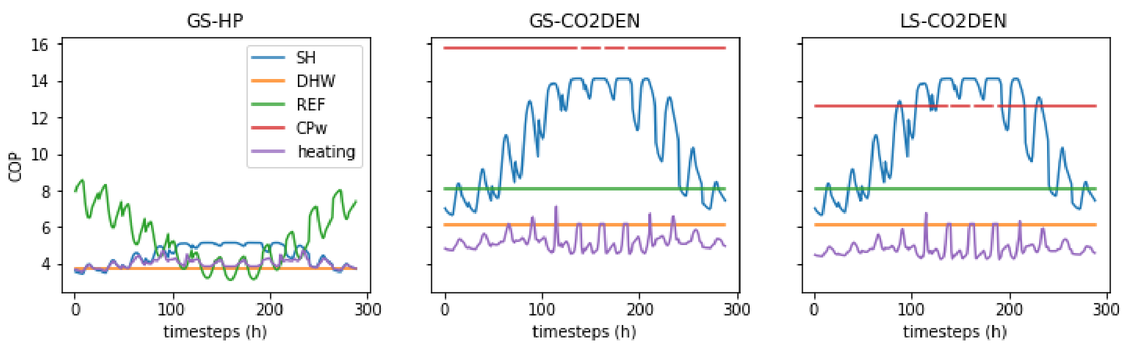

Figure 29: Comparison of COP values for each timestep t and unit. The *cooling* and the *global* COP are not displayed for praticality reasons, given their very high values during free cooling

A direct way to compare the performance of the different conversion technologies is the coefficient of performance, which is simply given by the ration between the delivered heat Q and the consumed electricity E. If the temperatures of evaporation and condensation of a heat pump are fixed, the operating cycle is also fixed, and thus the COP value. However, modern HP can adapt the operating cycle to fit the varying heat demand temperature. This allows to strongly improve the COP, as well as the exergy efficiency. The COP values, calculated in each timestep, are shown in Figure 29. The heating heat pumps for SH and DHW are considerably higher in the CO2DEN. This is due to the "two stages" of the conversion technology: the heat is first furnished to the CO2 network by the CP and then brought up to the required temperature by the decentralized HP. The COP of the central plant is higher in the GS CO2DEN, being the evaporation temperature higher than in the heat exchange with the lake. The SH HP has COP that varies between 6 and 14. This is due to the fact that the temperature of the heat demand rises with the amount of heat required. Thus the COP of the HP is lower during winter. Moreover, the compression chillers in the GS-HP perform worse during summer, when they have to deliver heat to a higher ambient temperature, while the COP of refrigeration in the CO2DEN are constant, since heat is delivered the whole year to the CO2 network, which has at constant temperature.

The mean COP values for each technology are shown in Table 16. The GS-CO2DEN shows the best performance with a global COP of 6.1. The LS-CO2DEN follows with 5.6 and the GS-HP with 4.6. All the conversion technologies perform well, but the combination of the DX-GSHP central plant with the decentralized HP in the GS-CO2DEN obtains excellent results.

Table 16: COP values for the three technological variants of energy system

	GSHP	GS-CO2DEN	LS-CO2DEN
HP-SH	4.5	10.8	10.8
HP-DHW	3.8	6.2	6.2
HP-REF	5.4	8.1	8.1
HP-CP_{winter}	-	15.8	12.6
Heating	4.0	5.2	4.9
Cooling	19.1	50.4	50.4
Global	4.6	6.1	5.6

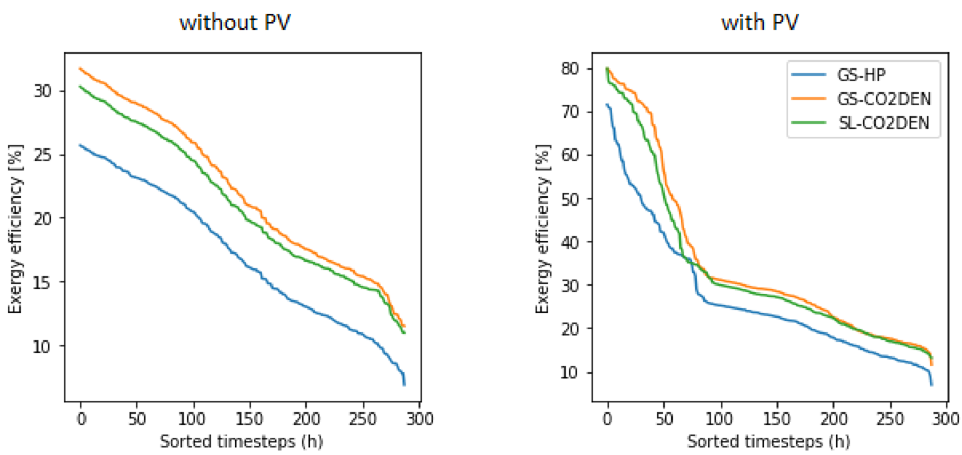

Figure 30: Comparison of exergy efficiencies calculated in each timestep - sorted in decreasing order - with the entire electricity demand on the left, and only with electricity bought from the grid on the right

The exergy values of supply and demand have been calculated for each conversion technology, as explained in Section 3.5. This analysis shows the real thermodynamic value of the required energy services, since not only the amount of heat is considered, but also the temperature level at which it happens. The exergy value of the demand is thus calculated in function of the varying ambient temperature and is the same for all technologies.

The difference in the exergy efficiency between the different conversion technologies is shown in Figure 30. On the left hand, the values are calculated without taking into account the domestic PV production of renewable electricity, while on the left hand this has been included in the calculation. It is clear to see that the GS-HP performs worse than than the CO2 DEN. The average exergy efficiency is of 17%, against 35% of the GS-CO2DEN. As it can be seen in Table 17, the exergy losses $\dot{L}_{\Delta T_{min}}$ due to the minimum approach temperature between the heat demand and the supply are small compared to the exergy losses occurring in the heat pumps $\dot{L}_{HP}$. The latter accounts for the COP of the heat pumps, which is as well dependent from the approach temperature with their respective heat sources. This explains the lower exergy efficiency of the GS-HP, for which its heat pumps require a much lower evaporation temperature, as discussed previously.

The reason for the high performance of the GS-CO2DEN, despite having two stages and thus some additional losses due to ΔT_{min} values, is the direct expansion of CO2. As shown in Section , the energy and exergy gain, with respect to the conventional system based on a secondary water loop, are indeed remarkable.

ref section

Even if for obvious reasons the exergy efficiency is considerably higher including the domestic PV production, the difference in performance between the different technologies does not change. This is explained by the fact that the self consumption values are very similar, as it can be seen in Figure 32 in purple, and the increase of efficiency is thus shared among all technologies. In this case the average exergy efficiency for the GS-HP is 27%, against 35% and 33% for respectively the GS- andn the LS-CO2DEN.

Table 17: Comparison of the exergy losses $\dot{L}$ and efficiencies η_{exergy}, with and without considering renewable PV production

-	units	GS-HP	GS-CO2DEN	LS-CO2DEN
$L_{\Delta T_{min}}$	[MWh]	77	47	47
L_{HP}	[MWh]	355	242	281
L_{tot}	[MWh]	432	289	327
η_{exergy}	[%]	17%	22%	21%
η_{exergy}^{PV}	[%]	27%	35%	33%

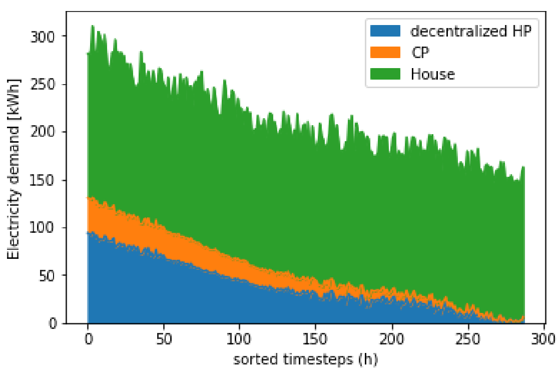

Figure 31: Electricity demand of GS-CO2DEN system grouped in categories, sorted in decreasing order

Figure 31 shows the shares of electricity consumption, on a sorted time axis. What is interesting

percentage of elcons reduction between technologies??

to note is the repartition of electricity consumption between the CP and the decentralized HP. E_{cp} represents around 10% of the global electricity consumption, and around 30% of the $E_{heat/cool}$.

5.2 Financial analysis

A financial analysis of the three conversion technologies is shown in Figure 32.

Given that in this work the cost of operation (OC) depend only from the consumed electricity (no consumption of gas or other resources), this is directly correlated to the global COP of the system. As seen above (see Table 16), GS-CO2DEN presents the highest coefficient of performance and thus also the lowest OC (dashed line), with $263'216[Euro/yr]$, and GS-HP the highest with $290'833[Euro/yr]$. The LS-CO2DEN presents an OC of $270'728[Euro/yr]$.

The investment costs are shown more in detail in the clustered columns. It is easy to note that the GS-HP has much lower upfront costs ($179'884[Euro/yr]$)than the GS-CO2DEN solution ($222'603[Euro/yr]$). Indeed, the reduction in the cost of the HP - which is due to the higher COP values - is compensated by a higher cost for the geothermal wells and the additional cost of the CO2 network. The first also originates from the higher COP values, for which a larger share of energy will come from the source, and thus require a larger capacity installed. The latter is intrinsic to the CO2DEN system, that requires a physical network of CO2 pipes to connect all the user. In the SL-CO2DEN there are obviously no costs related to the geothermal wells, but the cost for the water pipes that allow the water to be brought to the CP. Given the actual distance of the Eglantine district from the lake, this solution leads to much higher upfront costs than the competing technologies ($310'103[Euro/yr]$).

Despite the lower OC for the CO2DEN technologies, the total cost is clearly following the tendency of the IC, which present a larger difference. The GS-HP ends up being the cheapest variant with $470'717[Euro/yr]$, followed by the GS-CO2DEN with an only slightly higher cost of $485'819[Euro/yr]$. The SL-CO2DEN is the most expensive solution with $580'831[Euro/yr]$.

Self consumption and autarchy do not vary much between the technologies, because no storage technology has been taken into account. Indeed, any kind of storage - thermal, electrical or CO2 - would enable to adapt the consumption to profit from the cheap domestic produced energy, as well as to reduce peak demands. Moreover, despite of the optimizer choosing install the maximum possible amount of PV - which corresponds to the roof surface - for the three technologies, in order to reduce the OC, the amount of electricity produced is seldom larger than the total electricity demand of the district. Thus, the three systems have an autarchy of about 25 %, and a self consumption rate of around 75 %.

might be other reasons deciding, like space issue...

5.2.1 GS-HP

A parametric optimization of the costs of the reference energy system (GS-HP) is shown in Figure 33.

It can be seen that the biggest difference in investment and operating cost is due to the sizing of the PV. In fact, when constraining the investment costs, the model installs only a small share of PV, which increases the operational costs. On the contrary, a high share of PV increases the systems rate of auto-sufficiency, lowering the operational costs.

On the far right, the maximum allowed share of photovoltaic (PV) - set to twice the total roof area, which accounts for potential facades and free space PV - is reached. The operational are lowered thanks to a different handling of peak consumption. The optimal system installs a small share of electrical heater (R-EL) to cover peak demand, which allows to optimally size the heating heat pumps (HP-S, HP-DHW). In the last column on the right, the system chose not to install the electrical heater but installing larger heat pumps, which strongly increases upfront costs, but allows to further reduce the operational costs.

On the far left, the opposite phenomenon happens. To reduce upfront costs, the system chose to cover the heat demand almost entirely with help of the electric heater (R-EL), minimizing the size of the heating heat pumps (HP-SH, HP-DHW).

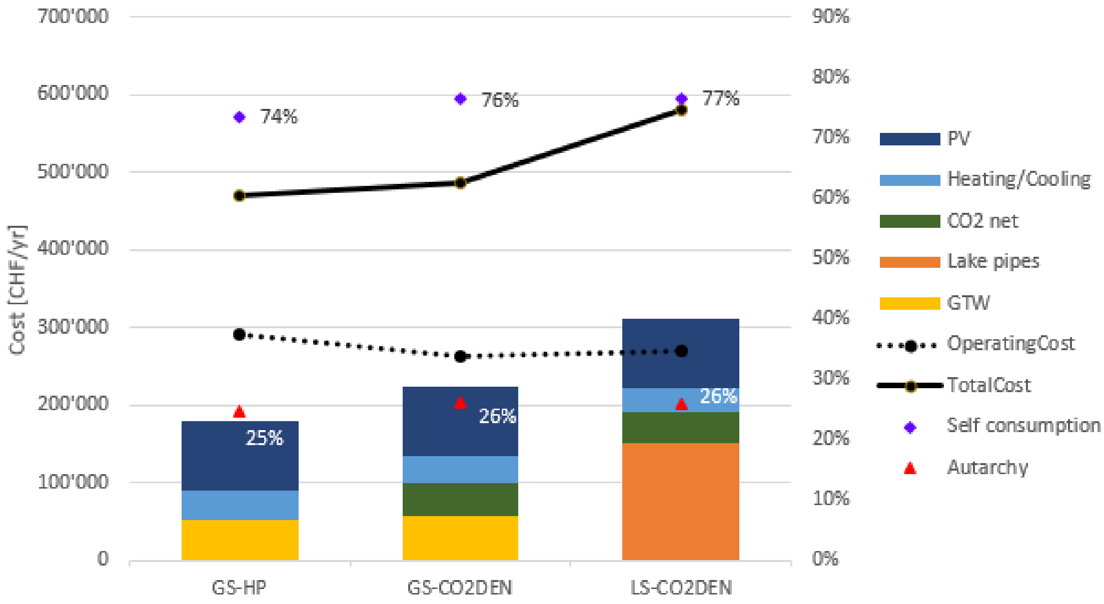

Figure 32: Cost comparison for the three different energy systems variants

The optimum, with respect to the total cost of the energy system, is in the very middle of the graph, between column 2 and 3. The optimum is analyzed in the following chapters.

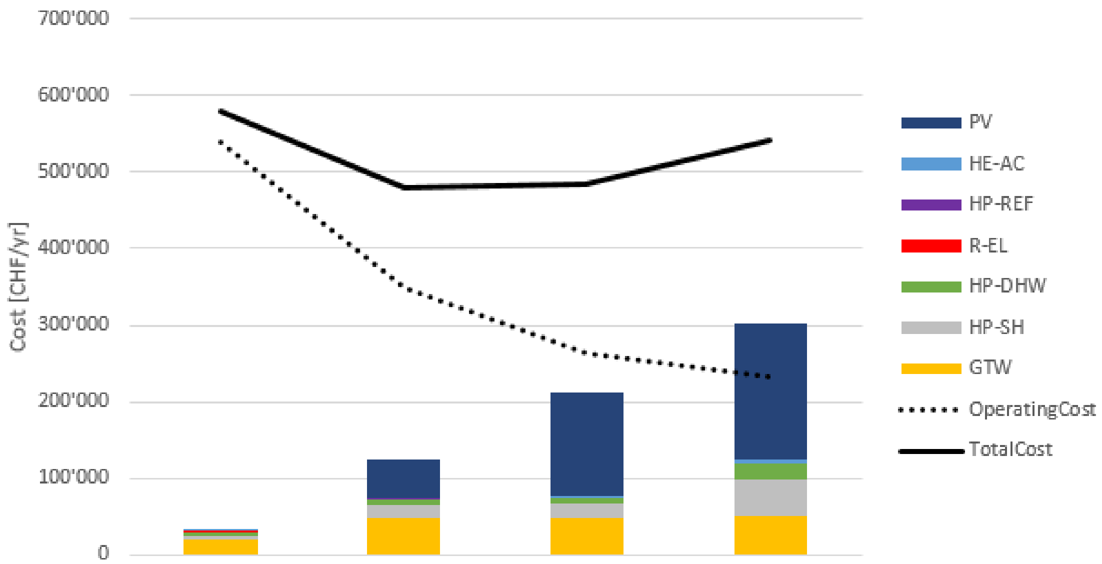

Figure 33: Parametric optimization of the reference energy system (GS-HP), showing the detailed investment costs, the operational cost and the total cost

5.2.2 GS-CO2DEN

A parametric optimization of the costs of the CO2 district energy system with ground sourced central plant (GS-CO2DEN) is shown in Figure 34.

The response of this system to the parametric optimization is very similar to the one of the GS-HP system. This means that the biggest difference in investment and operating cost is due to the sizing of the PV, while the extreme cases are determined by the ration between the electrical heater (R-EL) and the heating heat pumps (HP-SH, HP-DHW).

Also in this case the lowest total cost of the energy system is to be found in the very middle of the graph, between column 2 and 3. The optimum is analyzed in the following chapters.

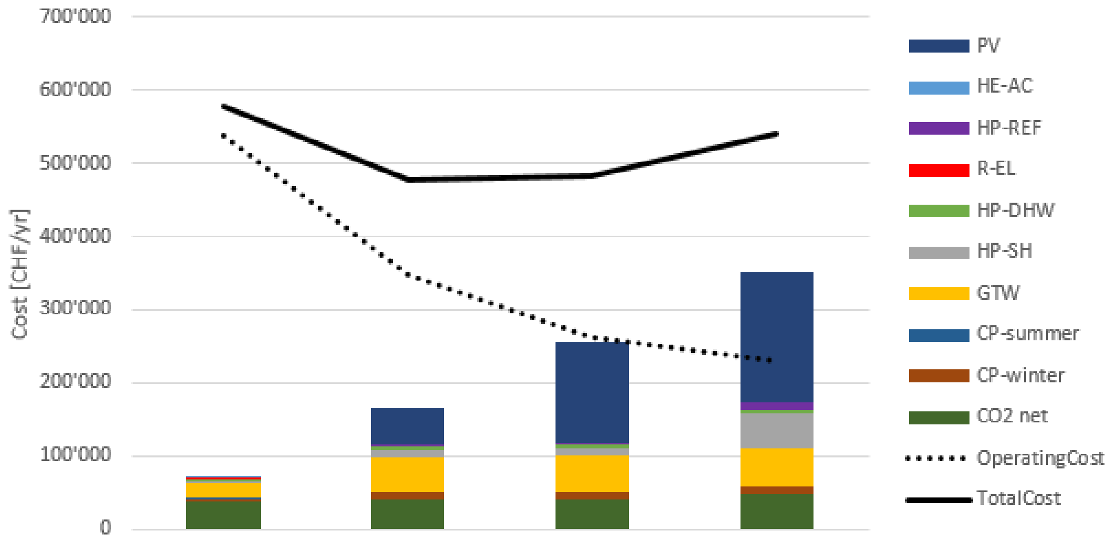

Figure 34: Parametric optimization of the ground sourced CO2 DEN (GS-CO2DEN), showing the detailed investment costs, the operational cost and the total cost

If we take the stable middle, isolate PV costs we obtain a share of network and HP correposnding to... This is shown in Table 18, in comparison with existing anergy networks in Switzerland.

Table 18: Cost comparison with existing anergy systems

		Eglantine	Anergienetz ETH Hönggerberg	Anergienetz Friesenberg
IC_{NET}	[%]	31.4 %	15.7 %	25.9 %
IC_{GTW}	[%]	42.0 %	32.7 %	23.5 %
$IC_{Heating/Cooling}$	[%]	26.5 %	49.2 %	50.6 %
Heating power	[kW]	592	8'000	3'930
Heating demand	[MWh/yr]	2'390	28'450	35'000
Cooling power	[kW]	84	6'000	3'500
Cooling demand	[MWh/yr]	33	26'200	80'000

It can be seen that the GS-CO2DEN system in the Eglantine district presents a much lower percentage of the investment cost $IC_{Heating/cooling}$ attributed to the heating and cooling equipment (HP-SH, HP-DHW, HP-REF, HE-AC) than two reference anergy networks in Switzerland.

One reason for this difference is most likely the size difference between the energy systems. In fact, the Eglantine system is drastically smaller than the one at ETH or in Friesenberg, which have a heating demand which is respectively 12 and 15 times bigger. The specific investment costs for building the network and drilling the geothermal wells decreases with size - for example the costs of digging to place a pipe underground won't be strongly correlated with the pipe diameter. On the contrary, the specific costs for the heat pumps will stay about the same, given that the size of the decentralized heat pumps will not increase, only its number.

On the other hand, it is not trivial to estimate the cost of building the CO2 network, given the lack of examples in the real world, and the resulting costs could be proven to be inaccurate. Also the sizing of the geothermal well, in order to account for yearly energy balance and recharge rate, and for the specific cost, according to depth and soil type would have to be verified and confirmed through further studies and simulations.

5.3 Ground temperature

A critical parameter for the efficiency of a ground sourced energy system is the ground temperature. As seen in Section 3.2, this temperature depends mainly on the depth, the temperature gradient in the given soil and the surface temperature. In other words, it is dependent from the location - including local climate and altitude - and the depth of drilling. In order to acknowledge the influence this temperature has on the system's performance, a sensitivity analysis has been performed. The results are shown in Figure 35

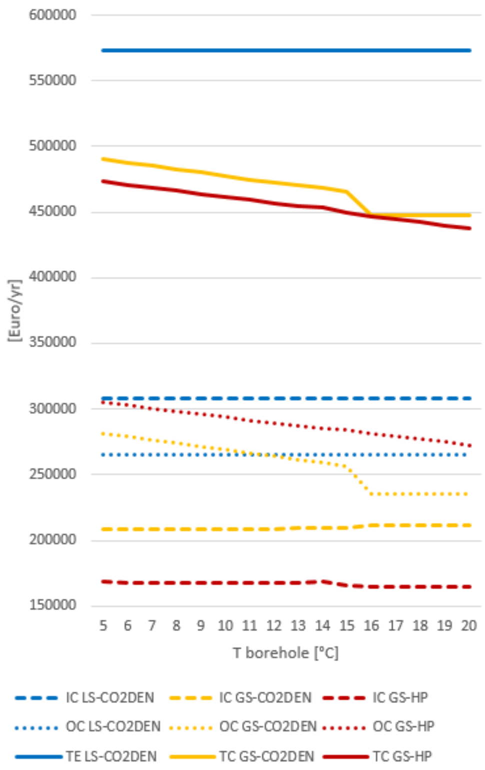

Figure 35: Cost comparison of variants in function of the borehole temperature

The GS-HP energy system seems to responds in a linear way to the temperature raise, as it can be expected, thanks to the lower required temperature raise for heating, which increases the COP of the system. In reality a small step can be identified between 14 and 15 °C, at which the IC drop and the OC rise. This step happens when the ground is not cool enough anymore to offer the option of free-cooling. The system is forced to use a refrigeration system instead, which increases the OC. However this utility is already installed, and thus the increase of IC_{HP-REF} is lower than the reduction of the obsolete IC_{HE-AC}.

The GS-CO2DEN energy system presents a more evident step in its response to the ground temperature. The reason lies in the use of the central plant, which, as described in Section , has different operating modes for cooling and heating. In fact, if the temperatures are either high or low enough, it can operate free-cooling or free-heating. In any other case, it operates in cooling and/or heating HP mode. In this case the step happens at $T_b \geq 16$°C, for which the CP can source heat directly from the ground without the need of a heat pump, which drastically reduces the operational costs.

write and reference model with if conditions

For obvious reason, while GS-CO2DEN and GSHP respond similarly to the variation in the bore temperature, the LS-CO2DEN presents constant costs. In fact the system is not dependent from the ground temperature and is represented on the graph for sake of comparison. It can be seen that $OC_{LS-CO2DEN}$ performs better, in terms of operating costs, than the GS-HP at any ground temperature in the studied interval. It also performs better than the GS-CO2DEN for temperatures below 10 °C. The lake distance in the Eglantine district is 1500m , which results in very high investment costs, precluding the competitiveness of this solution, in the given conditions.

Assuming uniform soil and maintaining a constant heat capacity, a higher borehole temperature would imply drilling a smaller number of wells with greater depth. In other words, the geothermal model described in Section 3.2 simply models the heat capacity and the investment cost per meter well. It is thus not able to properly account for advanced correlations between heat capacity, cost function and well depth.

Nevertheless, this sensitivity analysis gives an idea of the global behavior response of the different conversion technologies to the ground temperature. This can be very helpful to estimate the performance of either system, in function of the geographical location, latitude and altitude.

5.4 Lake distance

As it has been seen in the previous paragraphs, the LS-CO2DEN presents competitive OC. Avoiding geothermal drilling can thus represent a big advantage, through the reduction of upfront costs. Pressure losses as well as the energy for pumping have been neglected, so the cost of the water pipes is mainly dependent on the distance of the lake water. Thus the threshold for the distance of the lake can be calculated, for which the LS-CO2DEN system to present a lower total cost than the GS-CO2DEN system.

This threshold temperature varies in function of the ground temperature, and it has been calculated accordingly. The resulting thresholds are plotted on Figure 36. This helps choosing between using the lake or the soil as a heat source, knowing the mean ground temperature and the distance from the lake water.

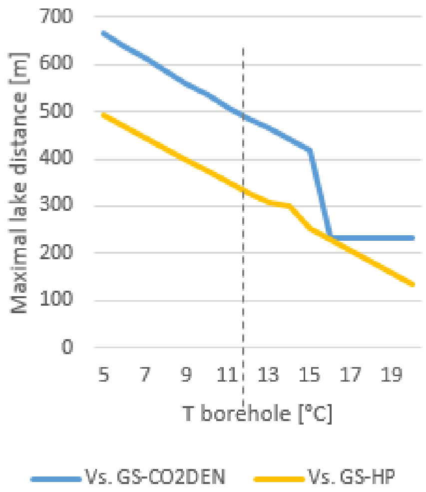

Figure 36: Maximum distance of lake for which the total costs are lower than the two other energy systems, in function of the ground temperature $T_{borehole}$

wrapfig

At $T_{borehole}$ = 12°C, as in the Eglantine district, the LS-CO2DEN would be a financially interesting solution against GS-HP and GS-CO2DEN if the distance to the lake is respectively shorter than 328 and 484 meters.

5.5 External heat source

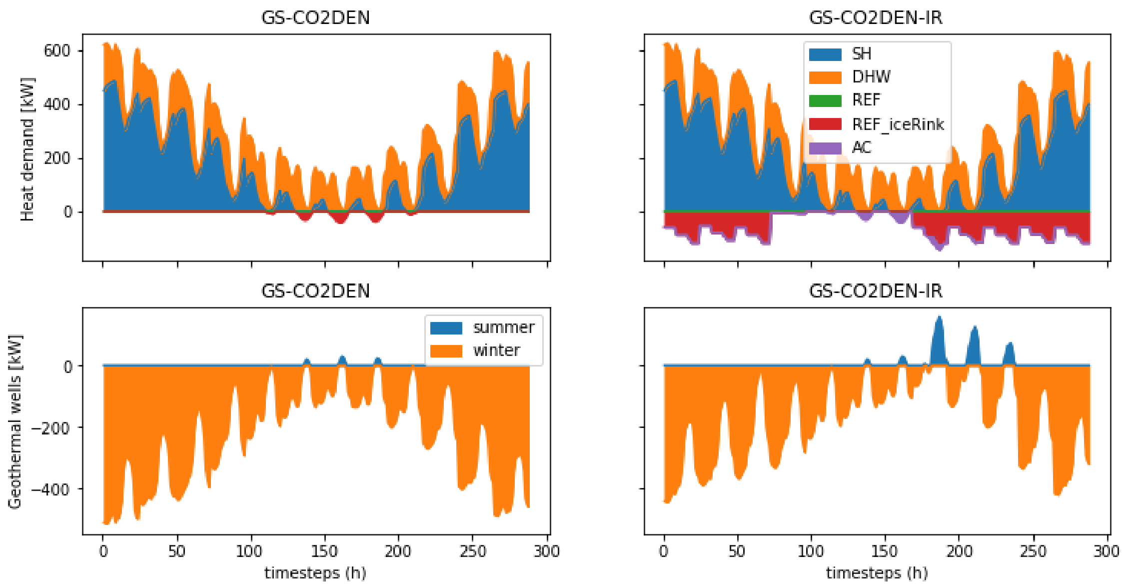

Figure 37: Heat supplied (above) and heat source use (below)

The integration of large external heat sources, as for example an ice rink, is very interesting for this technology, since it allows to recover heat, reducing the load of the CP, as well as for the heat source. It has been assumed that the existing facility already exists and thus its energy demands are not included in the model. The external heat source is purely considered as a free heat source.

The added heat demand is shown in the upper part of Figure 37 in red. This refrigeration demand will be inject heat into the CO2, balancing out the heat extracted from it, in order to satisfy the heating demand. This translates in a lower amount of heat that has to be furnished by the CP - reducing the total energy demand of the system -, which in turn will require less heat to be extracted from the heat source - reducing the needed source capacity. This can be identified in the lower part of Figure 37, where the orange area corresponds to the amount of heat that is extracted from the source, throughout the year.

In fact, the integration of the ice rink lowers the electricity demand of the heating/cooling facility from $471'500$ to $433'900[kWh/yr]$, for the same amount of heat demand (the ice rink has only been considered as a heat source and is not included in the heat demand of the system). Therefore, the global COP raises from 6.12 to 6.73.

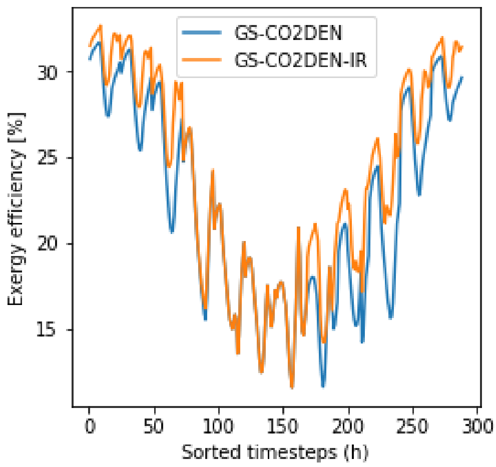

Figure 38: Comparison of exergy values of the GS-CO2DEN technology with and without the integration of the ice rink (IR)

From an exergy point of view, the integration of the external heat source replaces a share of the exergy value of the electricity. This translates in a higher exergy efficiency for those timesteps in which the external heat source is available, as shown in Figure 38. The mean exergy efficiency increases from 22.4% to 23.7%.

However, as it had been analyzed in Figure **??**, the electricity demand of the CP corresponds to about 30% of the demand of the heating/cooling facilities. This means that even a system having a perfectly balanced heating and cooling demand would not be able to reduce its OC of more than 30%, since, as far as the temperature of the CO2 network remains constant, the operating conditions of the decentralized heat pumps remain unchanged too.

An analysis of the economic differences caused by the integration of the ice rink is shown in Figure 39. As discussed above, the additional heat reduces the required heat from the GTW, reducing its IC, and reduces the workload of the CP, resulting in lower OC. On the other hand, the integration of the external heat source requires the installation of additional CO2 pipes, which has an impact on the upfront costs. In this particular case, it can be seen that the balance of these difference is negative, i.e. the total cost of the GS-CO2DEN is lower if the ice rink is connected.

Nevertheless, it is important to account for uncertainties bound to the external heat source. For example for an ice rink, the replacement of the obsolete and inefficient cooling facility, or an improvement in the facility management, can drastically reduce its energy. Same for other

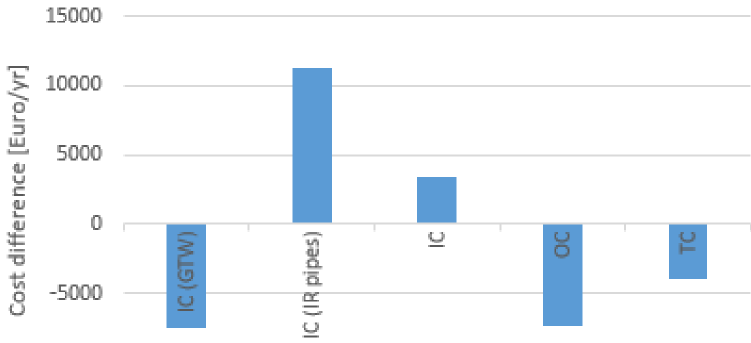

Figure 39: Cost difference of the GS-CO2DEN with and without ice rink. Positive values (+) reflect a higher, and negative values (-) a lower cost originated by the IR integration.

potential heat sources as industrial processes, which can be improved or replaced over time. This should be considered in the inclusion of external heat source, since a reduction, or the absence, of the additional heat could threaten the functioning of the system.

5.6 Optimization of energy demand

The Eglantine district is composed for 97% of buidlings dedicated to residential use (see Section 4.1), resulting in a very low cooling and refrigeration demand. It is now legitimate to wonder how the different energy systems would perform in a different district, i.e. with a different building use and thus a differently composed energy demand. In this chapter, it will be tried to answer this question, finding out the optimum district composition for the performance of a GS-CO2DEN system.

As per Table 6, the building categories are:

1. Housing
2. Retail
3. Restaurant services
4. Indoor swimming pool

For sake of simplicity, among the categories shown in Table 6, the two most common and diverse - i.e. presenting the most different energy demand - have been chosen: (1) Housing -H and (2) Retail - R.

A sensitivity analysis has been performed on a district composed by those two categories. The energy demand resulting from the different combinations of the above mentioned categories is shown in Figure 40. At the far right the energy demand resulting from a district composed by 100% of retail buildings, with a decreasing share towards the left, in steps of 25%. The last column on the left is given by the Eglantine district, as a reference. It is clear to see that the retail building has a high cooling demand during summer months, with demand peaks that are around 4 times the heating demand peaks. Moreover, while the space heating demand remains very similar, the hot water demand decreases considerably.

Table 19 shows the COP values for the energy system throughout the different combinations of buildings use. The $COP_{heating}$ increase is due to the decreasing share of DHW, which is heated with a lower COP. The increase in cooling, and thus the strong increase in the global coefficient of performance is due to the fact that the biggest share of the cooling demand can be satisfied with free-cooling. These variations are reflected in the decrease of electricity consumption, shown in Figure 40.

needed figure of source?

wrapfig

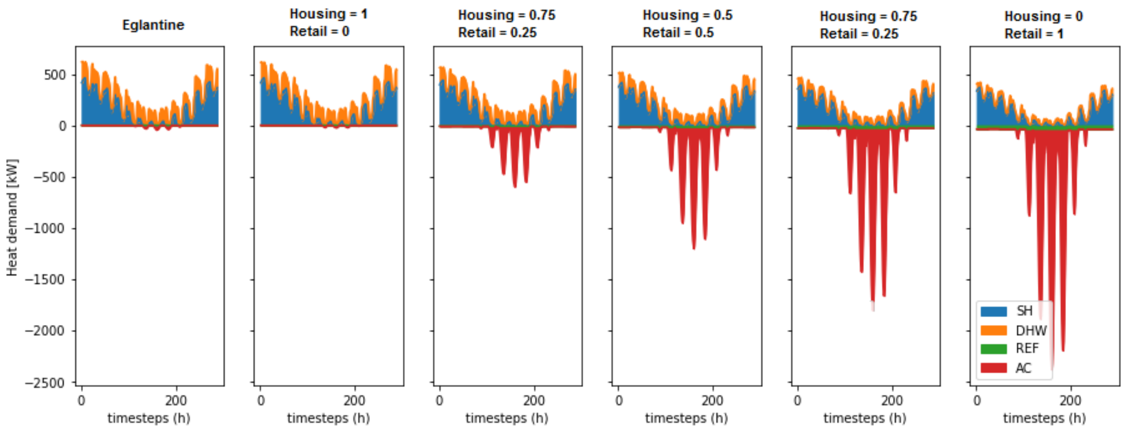

Figure 40: Comparison of the energy demand (power) for the different use of buildings throughout the year

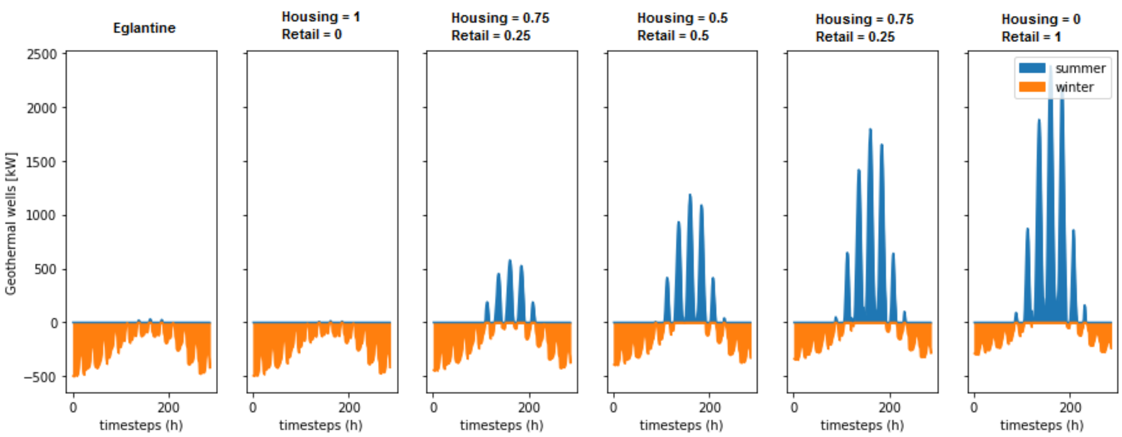

Figure 41: Comparison of the energy demand (power) of heat extracted (WINTER) of injected (SUMMER) into the boreholes

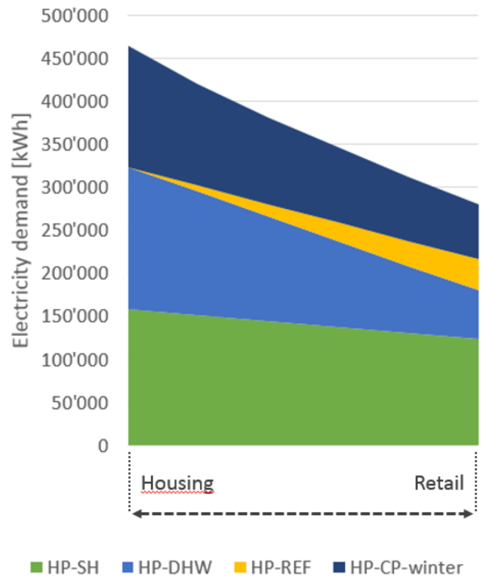

Figure 42: Electricity demand in function of the building use composition

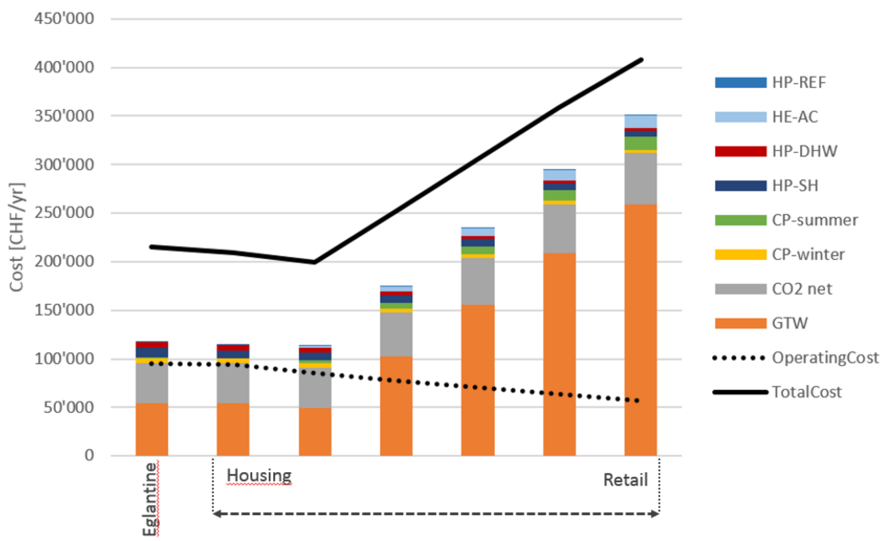

Figure 43: Cost comparison for different combinations of *housing* and *retail* building use, with the Eglantine district as a reference in the first column. The stacked columns show the investment costs.

Table 19: Comparison of energy demand and energy performance of the different combination of building use

		Eglantine	H1 / R0	H0.8 / R0.2	H0.6 / R0.4	H0.4 / R0.6	H0.6 / R0.8	H0 / R1
$Q^{+}_{heating}$	[MWh]	2'402	2'347	2'1614	1'976	1'790	1'603	1'426
$Q^{+}_{cooling}$	[MWh]	39	20	549	1'113	1'677	2'241	2'777
$Q^{netBalance}_{GTW}$	[MWh]	-1'887	-1'863	-1'195	-482	234'	951	1'632
$COP_{heating}$	[-]	5.1	5.1	5.4	5.7	5.9	6.1	6.3
$COP_{cooling}$	[-]	63.1	52.3	72.8	73.7	74.1	74.2	74.3
COP_{global}	[-]	5.9	5.5	14.7	22.3	29.3	36.3	43.6

Figure 43 shows the resulting costs, for the different scenarios. The decrease linearly, with the increase of the share of retail use. This is due to the smaller heating demand. The increasing cooling demand is essentially satisfied with free-cooling, which does not influence the operating cost. However, the increasing amount of energy that has to be dissipated in the ground has a big impact on the investment cost, since the model sizes them in order to satisfy the peak cooling power, which is around 2000 kW for a retail composed district. In comparison, the peak heating demand in the Eglantine district sums up to 500 kW. Therefore, the increase in the IC is much bigger than the decrease of OC.

In theory, the amount of heat extracted and injected in the ground should also be taken into account in the sizing of the GTW. Indeed, the a geothermal field can be used as a heat storage between the seasons. In Table 19 the net heat balance over a year is shown for each combination of district use. Thus, the fact that the model in this work sizes the GTW exclusively on the peak demand, is probably resulting in an overestimation of the investment costs for the GTW.

The optimum combination of the district composition, in terms of total cost, is to be found in low shares of retail, where the cooling demand allows to partly compensate the heating demand - thus reducing the operation cost - without increasing the peak demand for the GTW.

To find the precise value, a model that lets the solver choose the composition of the district has been implemented. This requires an additional set of constraints, which ensures that the chosen composition is maintained throughout all the timesteps:

$$f_{h,t} = f_{h,t+1} \ \forall \ t \in T, \ h \in H \tag{78}$$

where $f_{h,t}$ is the sizing variable of unit h in timestep t (see Section 2.5) and H is a subset of units U, corresponding to the above mentioned building categories.

Every unit h in H has been sized to the total ERA of the Eglantine district. Thus, in order to have comparable results, the next constraint ensures that the share of all h sum up to the size of the Eglantine district:

$$\sum_{h}^{H} f_{h,t} = 1 \ \forall \ t \in T, \ h \in H \tag{79}$$

The combination presenting the lowest total cost is found to be at:

$$f_{Retail} = 0.134$$

$$f_{Housing} = 0.866$$

Now that the response to a variation in the ground temperature has been studied, and that the performance of the system has been studied in function of different energy demands, it would be very interesting to know how the two parameters might be correlated between each other. In other words, it would be interesting to study the variation of the optimum combination of building use, in function of the borehole temperature. To do so, a sensitivity analysis has been performed on those two parameters, for the GS-HP and for the GS-CO2DEN.

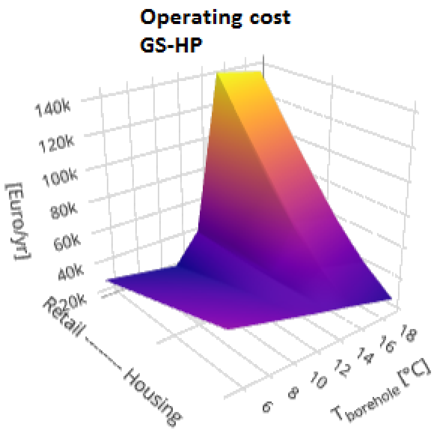

Figure 44: Operating costs in function of the borehole temperature and the building use in the district, using GS-HP technology

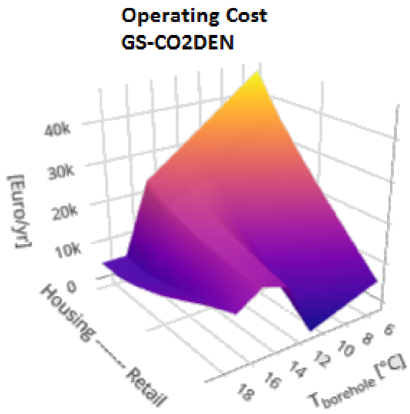

Figure 45: Operating costs in function of the borehole temperature and the building use in the district, using GS-CO2DEN technology

To evaluate the system's performance, it has been chosen to analyze the operating costs. Given that they are directly proportional with the global COP of the energy system, they give a very good indicator of the operating conditions. To do so, the electricity consumption of the houses has been neglected. The results are shown in Figures 44 and 45. It has to be noted that, for sake of visibility, the axis have been inverted between the two graphs. Moreover, the z axis is scaled differently.

Let's start looking at 44, the performance of the GS-HP. The temperature response to a *housing* composition is linearly decreasing with the temperature increase. This is due to the increase of COP in the decentralized HP, given the lower temperature rise to harvest heat from the ground. When moving towards a *retail* composition, i.e. introducing an increasing space cooling demand while lowering heating demand, the general plane has a decreasing slope, due to the lower heating demand. However, a strong increase appears for temperatures above 14 °C. The reason for that, is that the free cooling temperature threshold has been reached, requiring the use of the air cooled refrigeration system instead. This obviously engenders a considerable increase in electricity consumption, reflected in the operating cost.

The GS-CO2DEN, shown in Figure 45, shows a similar response to the temperature increase for *retail* composition, with a stronger drop once the temperature rises to the free heating threshold. This scenario had already been discussed in the previous sections. Now it is interesting to see what happens when moving towards *retail*. The COP at very low $T_{borehole}$ increases - thus the OC decrease - linearly with the decreasing share of heating demand and the increasing demand of free cooling. At very high $T_{borehole}$, on the contrary, the COP decreases - and OC increase - linearly with the increasing temperature drop that the refrigeration system has to perform in order to satisfy the cooling demand, which can not be free cooled. Nevertheless, the originated electricity consumption in this point is drastically lower than for the GS-HP, due to the much lower condensation temperature. In the temperature response for a purely *retail* district, it is very easy to see the different operating conditions of the CP, described in Section **??**. ref section CP

In general, the GS-CO2DEN achieves the highest energy performance, by being as close as possible to the free heating/cooling threshold temperatures, without crossing it. Depending on the demand, it will be more efficient to be on one side or the other of the thresholds, in order to use the more needed free energy. It has to be noted that the GS-CO2DEN performs better than the GS-HP for any given combination.

6 Conclusion and outlook

District energy systems have a high potential to improve the energy and exergy efficiency of urban heating and cooling systems. A particularly promising technology uses CO2 as a working fluid to exchange heat between buildings and a network of conversion technologies. A thermo-economic analysis of the technology has been performed, focusing on a test case district near Lausanne, the Eglantine district. This district composed of 13 buildings, with a total ERA of 43'350 m^2, and will host around 1'500 people. The building affectation is per 97% dedicated to housing, presenting a total heating demand of 2'350 MWh/yr.

Three main energy conversion technologies have been considered, for the supply of the heating and cooling demand. The first one consist in a state of the art, modern energy system, based on decentralized geothermal heat pumps (GS-HP), in combination with geo-cooling and air-cooled refrigerators. This is a common choice among new built district and houses. The other two, are CO2 based district energy networks, connected to a set of decentralized heat pumps, and a centralized heat pump to balance out the heat of the network with the environment. One of them has the central pump exchanging heat with a geothermal field (GS-CO2DEN), while the other exchanges heat with the lake water (SL-CO2DEN). The different technologies have been modeled accurately, in order to have the most realistic and impartial evaluation and comparison.

Results showed that the best performing technology is the GS-CO2DEN, with a global COP of 6.1 and an exergy efficiency of 22%, which is a considerable improvement with respect to the GS-HP that has a global COP of 4.6 and an exergy efficiency of 17%. This improvement is mainly due to the technology chosen for the central plant. In fact traditional geothermal heat pumps exchange heat with the ground through a secondary water loop, which is the case in the GS-HP. The CO2 network offers the possibility to expand the refrigerant directly into the ground. This cuts the need of an additional heat exchanger and, through the use of latent heat, avoids the additional temperature rise needed in the water loop. At last, but probably most relevant, liquid CO2 presents a much greater heat tranfer coefficient than water, reducing the needed minimum approach temperature to exchange with the ground from 14°C to 6.8 °C. Despite the lower compressor efficiencies for CO2, these measures considerably reduce exergy losses and improve the COP. The LS-CO2DEN has a slightly lower performance - global COP of 5.6 and exergy efficiency of 21% -, due to the lower temperature of the heat source.

Despite having the lowest COP, and thus the highest operating cost, the GS-HP presents the lowest total cost, with 470'717[Euro/yr]. The reason is straightforward: the reduction in operating cost do not compensate the upfront cost of the CO2 network, which has a total cost of 485'819 [Euro/yr]. Given the high distance to the lake (1'500 [m]), the LS-CO2DEN presents the highest total cost, with 580'831 [Euro/yr]. A sensitivity analysis on the lake distance has shown that this technology is cheaper than the others, if the lake water is at less than 328 [m]. Thus the arguments to opt for a CO2 network technology might not be purely financial. In fact, in cities an important argument is that often it might not be possible to drill boreholes for each building, since the space is simply not available.

To extend and improve these analysis, it would be necessary to implement storage technologies. In fact, in the actual model no storage technologies have been taken into account. This would enable to improve the sizing of the equipment, and also the integration with the domestic PV production. Especially, it would be interesting to analyze the possibility to store vapor and liquid CO2, which achieves the same effect as a battery or another heat storage. If investment cost and required storage volume are proved to be feasible and competitive, this form of storage could represent a key argument in favor of the CO2DEN technology.

Moreover, another crucial aspect for the improvement of the presented model, are the geothermal wells. Ideally, a model should be developed, capable of accounting for the temperature gradient of the soil in function of depth, as well as the varying heat transfer coefficient of CO2 during the different phases of the evaporation in the ground pipe [**?**, **?**]. This model should also account for heat capacity of the soil and its recharge rate[**?**, **?**, **?**], which would allow for geothermal heat storage or borehole regeneration.

Such a model would allow to improve the equipment sizing, as well as to better model the borehole's operating temperature and its dependency on the depth of the well.

References

7 Anergy nets Switzerland

Table 20: District energy systems in Switzerland

	Anergienetz ETH Hönggerberg	**Jardins de la Pâla**	**Suurstoffi-Areal**	**Anergienetz Friesenberg (FGZ)**	**CAD La-Tour-De-Peilz**	**Anergienetz-Visp**	**Genève-Lac-Nations (GLN)**
Location	Zürich	Bulle	Rotkreuz	Zürich	La-Tour-de-Peilz	Visp	Genève
Year of construction	2012 - 2026	2012 - 2020	2010 - 2020	2011-2050	2013 - 2015	2007 - heute	2008 - 2016
Type	¡ 20 °C	¡ 20 °C	¡ 20 °C	¡ 20 °C	¡ 20°C	¡ 20 °C	¡ 20 °C
ERA [m2]	475’000	65‘000	172’421	185’000	24 Buildings	160’000	840’000
Use	School Residential	Residential Commercial Industry	Residential Administration Commercial Catering School	Residential Computation	Residential Administration	Residential Industry	Residential Administration School
Status	Partly built	Partly built	Partly built	Partly built	Built	Built	Built
				Data Energy Consumption			
Inst. Heating capacity [kW]	8’000	2’000	6’732	3’930	10’000	3’467	4’300
Heating demand ’[MWh/a]’	28’450	3’100	10’619	35’000	812	8’737	5’000
Inst. Cooling capacity [kW]	6’000	1’000	2’327	3’500	None	2’600	16’200
Cooling demand ’[MWh/a]’	26’200	650	2’364	80’000	None	3’380	20’000
Heat source	Laboratories waste heat +HP	Groundwater+HP	Waste heat buildings + PVT (solar th.) +HP	Waste heat data center+HP	Lake water +HP	Inudstrial waste heat + HP	Lake water +HP
Heat storage	Geothermal well field (431 at 200m)	Groundwater 12°C	Geothermal well field (215 at 150 m, 180 at 280m)	Geothermal well field (332 at 250m)	None	None	None
				Network data			
Network length [km]	1.5	0.85	2.5	1.5	4.1	4.2	6
Heating pipeT	24 °C - 8 °C	12 °C - 9 °C	25 °C - 8 °C	28 °C - 8 °C	20 °C - 6 °C	18 °C - 8 °C	17 °C - 5 °C
Cooling pipeT	4 °C - 20 °C	4 °C - 17 °C	4 °C - 17 °C	4 °C -24 °C	2 °C - 16 °C	4 °C - 16 °C	5 °C - 12 °C
Pipe diameter [mm]	DN 560	75 - 250	60 - 400	400 - 500	400 -700	DN 400	100 -700
Number of pipes	3	2	2	2	2	2	2

Table 21: District energy systems in Switzerland

	Anergienetz ETH Hönggerberg	**Jardins de la Pâla**	**Suurstoffi-Areal**	**Anergienetz Friesenberg (FGZ)**	**CAD La-Tour-De-Peilz**	**Anergienetz-Visp**	**Genève-Lac-Nations (GLN)**
				Financial data			
Tot. investments '[Mio.CHF]'	37	6	n/a	42.5	32	1.26	33
Interest rate[%]	3.9 - 6.7		n/a	n/a	6.4	5.8 - 8	n/a
Lifespan [a]							
Pipes	50	30	40	50	50	40	n/a
Storage	50	None	80	50	None	None	n/a
Heating unit	20	15	20	20	25	20	n/a
Cooling unit	20	15	20	20	25	20	n/a
Cost of energy '[Rp./kWh]'	7.7 (Heating +cooling)	5.85 – 8 (at the moment only heating)	n/a	18 (Heating)	19.8 (at the moment only heating)	22.9 (Heating + cooling)	n/a
Tot. COP of heating	7.2	4.4	n/a	5.2	n/a	n/a	n/a
Tot. COP of heating (incl. Pumps...)	5.8	2.7	2.7	4.1	3.5-4	4	6.5
Tot. EER of cooling	30.1	n/a	n/a	n/a	n/a	n/a	n/a
Tot. EER of cooling (incl. Pumps...)	6.9	12.1	n/a	n/a	n/a	n/a	n/a